Alma Mater Studiorum · University of Bologna

Department of Physics and Astronomy

Master Degree in Physics

THESIS TITLE

Supervisor:
Prof. Enrico Giampieri
Co-Supervisor:
Dott.sa Lidia Strigari

Submitted by:
Lorenzo Spagnoli

Academic Year 2020-2021

Dedication...

Abstract

Contingency table per le segmentazioni sostituibili

	ICU Admission	
	0	1
Death		
0	7	2
1	8	1

Contingency table per le segmentazioni brutte o dubbie

	ICU Admission	
	0	1
Death		
0	32	4
1	11	2

Since the start of 2020 *Sars-COVID19* has given rise to a world-wide pandemic. In an attempt to slow down the fast and uncontrollable spreading of this disease various prevention and diagnostic methods have been developed. In this thesis, out of all these various methods, the attention is going to be put on Machine Learning methods used to predict prognosis that are based, for the most part, on data originating from medical images. The techniques belonging to the field of radiomcs will be used to extract information from images segmented using a software available in the hospital that provided the clinical data as well as the images. The usefulness of different families of variables will be evaluated through their performance in the methods used, namely Lasso regularized regression and Random Forest. Dimensionality reduction techniques will be used to attain a better understanding of the dataset at hand. Following a first introductiory chapter in the second a basic theoretical overview of the necessary core concepts that will be needed throughout this whole work will be provided and then the focus will be shifted on the various methods and instruments used in the development of this thesis The third is going to be a report of the results and finally some conclusions will be derived from the previously presented results. It will be concluded that the segmentation and featue extraction step is of pivotal importance in driving the performance of the predictions. In fact, in this thesis, it seems that the information from the images adds no significant information to that derived from the clinical data. This can be taken as a symptom that the more complex *Sars-COVID19* cases are still too difficult to be segmented automatically, or semi-automatically by untrained personnel, which will lead to counter-intuitive results further down the analysis pipeline.

Contents

Chapter 1

Introduction

Nowadays everybody knows of *Sars-COVID19* which, since the start of 2020, has made necessary a few world-wide quarantines forcing everybody in self-isolation. It is also well known that, among the main complications and features of this virus, symptoms gravity as well as the rate of deterioration of the conditions are some of the most relevant and problematic. In some cases asymptomatic or near to asymptomatic people may, in the span of a week, get to conditions that require hospital admission. This peculiarity is also what heavily complicates the triage process, since trying to predict with some degree of accuracy the prognosis of the patient at admission is a thoroughly complex task. In this thesis the aim will be to use data, specifically including data that cannot be easily interpreted by humans, to try various methods to predict a couple of clinical outcomes, namely the death of the patient or the admission in the Intensive Care Unit (ICU), while assessing their performance. These analyses will be carried out on a dataset of 434 patients with different variables associated to every person. A part of the variables, which will be called clinical and radiological, are defined by humans and are generally discrete in nature but mostly boolean. The most part of the available variables, however, will be image-derived following the approaches used in the field of radiomics. While the utility of clinical variables, such as age, obesity and history of smoking, is very straightforward it's interesting and helpful to understand the basis behind the utility of radiomic and radiological features. Generally speaking it's clear that images have the ability to convey a slew of useful images, this is expecially true in the medical field where digital images are used to inspect also the internal state of the patient giving far more detailed information than that obtainable by visual inspection at the hand of medical professionals. Among the ways in which *Sars-COVID19* can manifest himself the one that is most relevant to the scopes of this thesis pneumonia and the complications that stem from it. Some of these complications, which are not specific of *Sars-COVID19* but can happen in any pneumonia case, display very peculiar patterns when visualizing the lungs through CT exams. These patterns are due to the pulmonary response to inflammation which may lead to thickening of the bronchial and alveolar structures up to pleural effusions and collapsed lungs. Without going too much in clinical detail what is of interest is how these condition manifest themselves in the CT exams:

1. **Ground Glass Opacity(GGO)**:
   Small diffused changes in density of the lung structure cause a hazy look in the affected region. This complicates the individuation of pulmonary vessels.

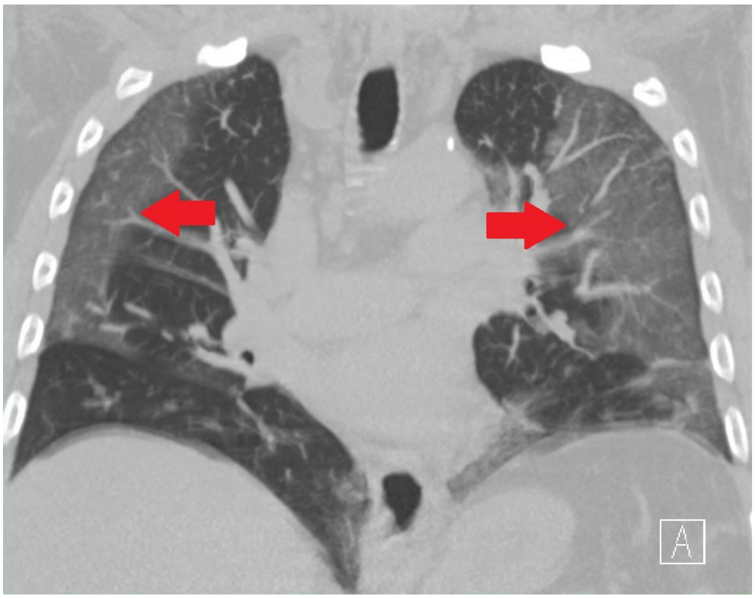

Figure 1.1: Example of GGO

2. **Lung Consolidations**:
   Heavier damage reflects in whiter spots in the lung as the surface more closely resembles outside tissue instead of normal air. The consolidation refer to presence of fluid, cells or tissue in the alveolar spaces

3. **Crazy paving**:
   When GGOs are superimposed with inter-lobular and intra-lobular septal thickening.

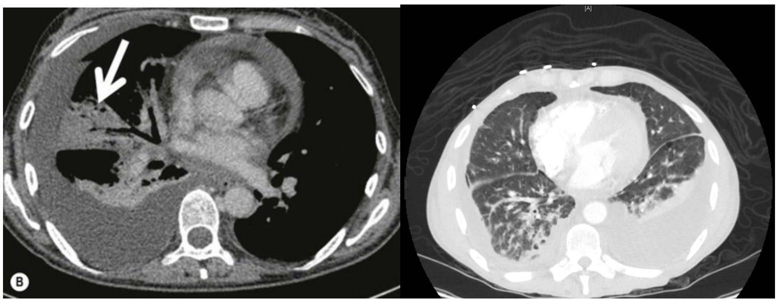

(a) a   (b) a

Figure 1.2: Differences between a collapsed lung (a) and pleural effusion(b)

4. **Collapsed Lungs and Pleural Effusion**:
   Both of these manifest themself as regions of the lungs that take the same coloring as that of tissue outside the lung. The main difference between the two is that collapsed lungs are somewhat rigid structures, they can occur in singular lobes of the lung and stay where they occur. Pleural effusions, however, are actually fluid being located in the lung instead of air. As such these lesions usually are located 'at the bottom' of the lung in which they happen and migrate to the lowest part of the lung according to the position of the patient.

Having these manifestation it's clear that they are mainly textural and intensity-like changes in the normal appearance of the lungs. However, whereas these properties can be easily described in a qualitative and subjective way, it's rather complex to describe them in a quantitative and objective way. The field of radiomics, when coupled with digital images and preprocessing steps which must include image segmentation, is exactly what undertakes this daunting task. Radiomics comes from the the combination of radiology and the suffix *-omics*, which is characteristic of high-throughput methods that aim to generate a large number of numbers, called biomarkers or features, as such it uses very precise and strict mathematical definitons to quantify in various ways either shape, textural or intensity based properties of the radiological image under analysis. Given the large numerosity of the features produced by radiomics it's necessary to analyze these kinds of data with methods that rely on Machine Learning and their ability to address high-dimensional problems, be it in a supervised or unsupervised way, in a rather fast and accurate way. Starting from these premises this thesis will be divided in a few chapters and sections. The first step will be taken by providing the general theoretical background regarding the aforementioned topics and techniques, this will be followed by a desscription of the data in use as well as a presentation of the analysis methods and resources used. Finally the results of the methods described will be presented and from them a set of concluding remarks will be set forth.

Chapter 2

Materials and methodologies

In this section there's going to be an explanation of the dataset as well as instruments and methodologies used to analyze it's properties, as such the first step is going to be an in depth discussion of the data available and a general overview of the final use. The following step is going to be a description of the preliminary work done to the data itself and to the results of this preliminary analysis in order to select the important features. The final step of this chapter is going to be an explanation of the methods used to derive the final results and to evaluate them.

2.1 Theoretical background

2.1.1 Medical Images

In this section the objective is to simply provide a set of basic definitions pertaining to images as well as a general introduction to the methods used to create said images. Firstly images are a means of representing in a visual way a physical object or set thereof, when talking about images it's common to refer specifically to digital images.

Definition 2.1.1 (Digital Image)**.** A numerical representation of an object; more specifically an ordered array of values representing the amount of radiation emitted (or reflected) by the object itself. The values of the array are associated to the intensity of the radiation coming from the physical object; to represent the image these values need to be associated to a scale and then placed on a discrete 2D grid. To store these intensities the physical image is divided into regular rectangular spacings, each of which is called pixel[1], to form a 2D grid; inside every spacing is then stored a number (or set thereof) which measures the intensity of light, or color,

[1] The term pixel seems to originate from a shortening of the expression Picture's (pics=pix) Element(el). The same hold for voxel which stands for Volume Element

coming from the physical space corresponding to that grid-spacing. The term digital refers to the discretization process that inherently happens in storage of the values, called pixel values, as well as in arranging them within the grid. It's possible to generalize from 2D images to 3D volumes, simply by stacking images of the same object obtained at different depths. In this context, the term pixel is substituted by voxel, however since they are used interchangeably in literature they will, from now on, be considered equivalent.

Generally pixel values stored as integers p$\in$ $[0,2^n$-1] with p,n$\in$ $\mathbb{N}$ or as p$\in$[0,1] with p$\in$ $\mathbb{R}$, the type of value stored within each pixel changes the nature of the image itself. A single value is to be intended as the overall intensity of light coming from the part of the object contained corresponding to the gridspace and is used for a gray-scale representation, a set of three[2] or four[3] values can be intended as a color image.

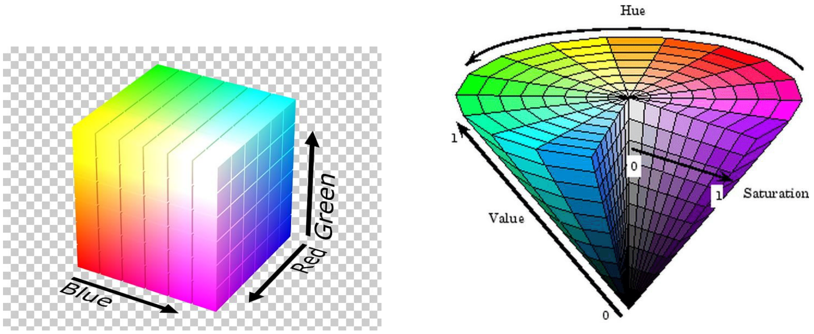

(a) RGB color space on a cube

(b) HSV cone

Figure 2.1: Examples of color spaces

There are a lot of possible scales for representation[4], which are sometimes called color-spaces, however the most noteworthy in the scope of this work is the Hounsfield unit (HU) scale.

Definition 2.1.2 (Hounsfield unit (HU))**.** A scale used specifically to describe radiodensity, frequently used in the context of CT (Computed Tomography) exams. The values are obtained as a transformation of the linear attenuation coefficient **??** of the material being imaged and, since the scale is supposed to be used on humans, it's defined such that water has value zero and air has the most negative value -1000. For a more in depth discussion refer to [11]

[2] The three values correspond each to the intensity of a single color, the most commonly used set of colors is the RGB-scale (Red, Green, Blue). Further information can be found by looking into Tristimulus theory[23]

[3] Same as RGB but with four colors, the most common scale is CMYK (Cyan, Magenta, Yellow, blacK)

[4] Besides RGB and CMYK 2.1a the most common color spaces are CIE (Commision Internationale d'Eclairage) and HSV fig:2.1b (Hue,Saturation and Value). Refer to [9] for further details

$$HU = 1000 * \frac{\mu - \mu_{H_2O}}{\mu_{H_2O} - \mu_{Air}} \tag{2.1}$$

The utility of this scale is in it's definition, since the pixel value depends on the attenuation coefficient it's possible to individuate a set of ranges that identify, within good reason, the various tissues in the human body: for example lungs are [-700, -600] while bone can be in the [500, 1900] range. A more in depth discussion of the topics relative to Hounsfield units is going to be carried out at a later point throughout this chapter, in the meantime it's necessary to clarify what are the most important characteristics of an image:

- Spatial Resolution: A measure of how many pixel are in the image or, equivalently, how small each pixel is; a larger resolution implies that smaller details can be seen better fig:2.2. Can be measured as the number of pixel measured over a distance of an inch ppi(Pixel Per Inch) or as number of line pairs that can be distinguished in a mm of image lp/mm (line pair per millimeter).
- Gray-level Resolution: The range of the pixel values, a classic example is an 8-bit resolution which yields 256 levels of gray. A better resolution allows a better distinction of colors within the image fig:2.2.

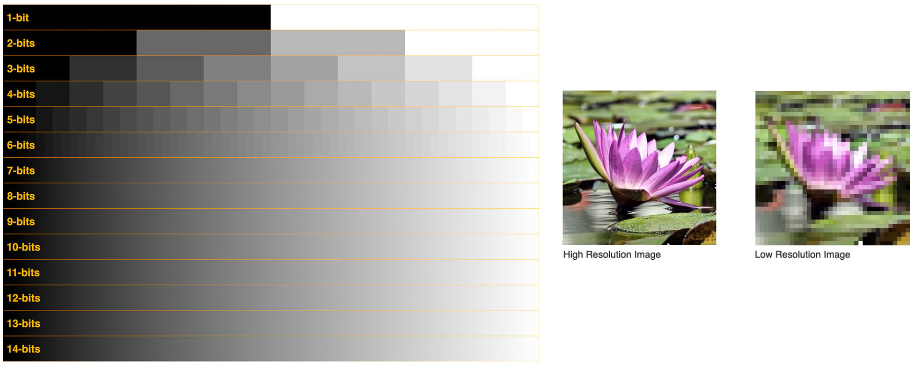

Figure 2.2: Example of visual differences in Gray-level (left) and spatial (right) resolution

- Size: Refers to the number of pixel per side of the image, for example in CT-derived images the coronal slices are usually 512x512. These numbers depend on the acquisition process and instrument but in all cases these refer to the number of rows and columns in the sampling grid as well as in the matrix representing the image.
- Data-Format: How the pixel values are stored in the file of the image. The most commonly used formats are .PNG and .JPG however there are a lot of other formats. In the context of this work, which is going to be centered on medical images, the most interesting formats are going to be the nii.gz (Nifti) and the .dcm (DICOM). The first contains only the pixel value information

hence it's a lighter format, it originates in the field of Neuroimaging[5], it is used mainly in Magnetic resonance images of the brain but also for CT scans and, since it contains only numeric information, it's the less memory consuming option out of the two. The second contains not only the image data but also some data on the patient, such as name and age, and details on how the exam was carried out, such as machine used and specifics of the acquisition routine. This format is heavier than the previous one and, for privacy purposes, is much more delicate to handle which is why anonymization of the data needs to be taken in consideration. For a thorough description of the DICOM standard refer to [1].

The format in which the image is saved depends on the compression algorithm used to store the information within the file. These algorithms can be lossy, in which case some of the information is lost to reduce the memory needed for storage, or lossless which means that all the information is kept at the expense of memory space. The first set of methods is preferred for storage of natural images, these are cases in which details have no importance, whereas the second set of methods is used where minute details can make a considerable difference such as in the medical field[6]. Given this set of characteristics it should now be clear that images can be thought of as array of numbers, for this reason they are often treated as matrices and, as such, there is a well defined set of valid operations and transformations that can be performed on them. All these operations and transformations, in a digital context[7], are performed via computer algorithms which allow almost perfect repeatability and massive range of possible operations. Given the list-like nature of images one of the most natural things to do with the pixel values is to build an histogram to evaluate some of the characteristic values of their distribution, such as average, min/max, skewness, entropy... . The histogram of the image, albeit not being an unambiguous way to describe images, is very informative. When looking at an histogram it's immediately evident whether the image is well exposed and if the whole range of values available is being used optimally.

[5] In fact Nifti stands for Neuroimaging Informatics Technology Initiative (NIfTI)

[6] A detailed description of compression algorithms is beyond the scopes of this thesis, for this reason please refer to [25] for more information

[7] As opposed to analog context, which would mean the chemical processes used at the start of photography to develop and modify the film on which the image was stored

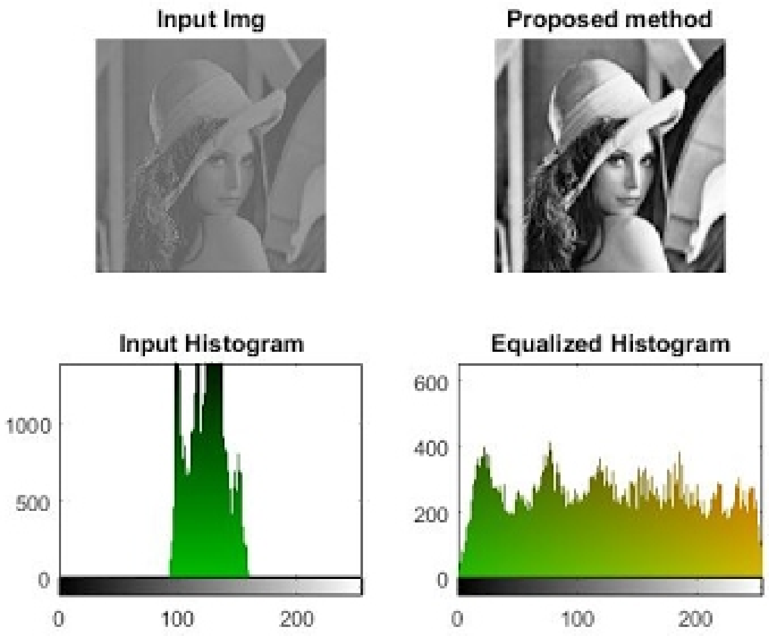

Figure 2.3: Example of differences in contrast due to histogram equalization

This leads us to the concept of *Contrast* which is a quantification of how well different intensities can be distinguished. If all the pixel values are bundled in a small range leaving most of the histogram empty then it's difficult to pick up the differences because they are small however, if the histogram has no preferentially populated ranges then the differences in values are being showed in the best possible way fig:2.3. Note also that if looking at the histogram there are two(or more) well separated distributions it's possible that these also identify different objects in the image, which will for example allow for some basic background-foreground distinction. Assuming they are being meaningfully used [8] all mathematical operations doable on matrices can be performed on images for this reason it would be useless to list them all. However, it's useful to provide a list of categories in which transformations can be subdivided:

1. Geometric Transformations involve the following steps:
   (a) Affine transformations: Transformations that can can be performed via matrix multiplication such as rotations, scaling, reflections and translations. This step basically involves computing where each original pixel will fall in the transformed image
   (b) Interpolation: Since the coordinates of the transformed pixel might not fall exactly on the grid it might become necessary to compute a kind of average contribution of the pixel around the destination coordinate

[8] For example adding/subtracting one image to/from another can be reasonably understood, multiplying/dividing are less obvious but still used e.g. in scaling/mask imposition and change detection respectively

to find a most believable value. Examples of such methods are linear, nearest neighbour and bicubic.

2. Gray-level (GL) Transformations: Involve operating on the value stored within the pixel, these can be further subdivided as:

   (a) Point-wise: The output value at specific coordinates depends only on the output value at those same specific coordinates. Some examples are window-level operations, thresholding, negatives and non-linear operations such as gamma correction which is used in display correction. Taken p as input pixel value and q as output and given a number $\gamma \in \mathbb{R}$, gamma corrections are defined as:

   $$q = p^\gamma \tag{2.2}$$

   (b) Local: The output value at specific coordinates depends on a combination of the original values in a neighbourhood around that same coordinates. Some examples are all filtering operation such as edge enhancement, dilation and erosion. These filtering methods are based on performing convolutions in which the output value at each pixel is given bu the sum of pixel-wise multiplication between the starting matrix and a smaller (usually 3x3 or 5x5) matrix called kernel. The output image is obtained by moving the kernel along the starting matrix following a predefined stride, when moving near the borders the behavour is defined by the padding of the image. Stride, kernel shape and padding determine the shape of the output matrix VALE LA PENA METTERE LA FORMULA E SPIEGARLO MEGLIO?.

   (c) Global: The output value at specific coordinates depends on all the values of the original images. Most notable operation in this category is the Discrete Fourier Transform and it's inverse which allow switching between spatial and frequency domains. It's worth noting that high frequency encode patterns that change on small scales whereas low frequencies encode regions of the image that are constant or slowly varying.

The aforementioned is surely not a comprehensive list of all that can be said on images however it should be enough for the scopes of this work.

Having seen what constitutes and image and what can be done with one it becomes interesting to explore how images are obtained. The following discussion is going to introduce briefly some of the methods used to obtain medical images, getting more in depth only on the modality used to obtain all the images used in this thesis which is Computed Tomography.

1. Magnetic Resonance Imaging (MRI): This technique is based on the phenomenon of Nuclear Magnetic Resonance(NMR) which is what happens when diamagnetic atoms are placed inside a very strong uniform magnetic field are subject to Radio Frequency (RF) stimulus. These atoms absorb and re-emit the RF and supposing this behaviour can somehow be encoded with a positional dependence then it's possible to locate the resonant atoms given the response frequency measured. Suffices to say that this encoding is possible however the setup is very complex and the possible images obtainable with this method are very different and can emphasize very different tissue/material properties. Nothing more will be said on the topic since no data obtained with this methodology will be used. More details can be found in [5]
2. Ultra-Sound (US): The images are obtained by sending waves of frequency higher to those audible by humans and recording how they reflect back. This technique is used mainly in imaging soft peripheral tissues and the contrast between tissues is given by their different responses to sound and how they generate echo. The main advantages such as low cost, portability and harmlessness come at the expense of explorable depth, viewable tissues, need for a skilled professional and dependence on patient bodily composition as well as cooperation.
3. Positron Emission Tomography (PET): In this case the images are obtained thanks to the phenomenon of annihilation of particle-antiparticle, specifically of electron-positron pairs. The positrons come from the β^+ decay of a radionucleide bound to a macromolecule, which is preferentially absorbed by the site of interest [9]. Once the annihilation happens a pair of (almost) co-linear photons having (almost) the same energy of 511 keV is emitted, the detection of this pair is what allows the reconstruction of the image representing the pharmaceutical distribution within the body. Once again there are a lot of subtleties that are beyond the scopes of this thesis, suffices to say that: firstly the exam is primarily used in oncology given the greater energy consumption, hence nutrients absorption, of cancerous tissue and secondly this technique can be combined with CT scans to obtain a more detailed representation of the internal environment of the patient

The last technique that is going to be mentioned is Computed Tomography however, given it's relevance inside this thesis work, it seems appropriate to describe it in a dedicated section.

[9] Most commonly Fluoro-DeoxyGlucose FDG which is a glucose molecule labelled with a ^{18}F atom responsible of the β^+ decay. In general these radio-pharmaceuticals are obtained with particle accelerators near, or inside, the hospital that uses them. They are characterized by the activity measured as decay/s $\doteqdot$ Bq (read Becquerel) and half-life $\doteqdot$ $T_{\frac{1}{2}}$ which is how long it takes for half of the active atoms to decay

X-ray imaging and Computed Tomography (CT)

It's well known that the term x-rays is used to characterize a family electromagnetic radiation defined by their high energy and penetrative properties. Radiation of this kind is created in various processes such as characteristic emission of atoms, also referred to as x-ray fluorescence, and Bremsstrahlung, braking radiation[10]. The discovery that "A new kind of ray" [26] with such properties existed was carried out by W.C.Roentgen in 1895, which allowed him to win the first Nobel prize in physics in the same year. Clearly the first imaging techniques that involved this radiation were much simpler than their modern counterpart, first of all they were planar and analog in nature, as well as not as refined in image quality. The first CT image was obtained in 1968 in Atkinson Morley's Hospital in Wimbledon. Tomography indicates a set of techniques[11] that originate as an advancement of planar x-ray imaging; these techniques share most of the physical principles with planar imaging while overcoming some of it's major limitations, main of which being the lack of depth information. X-ray imaging, both planar and tomographic, involves seeing how a beam of photons changes after traversing a target, the process amounts to a kind of average of all the effects occurred over the whole depth travelled. The way in which slices are obtained is called focal plane tomography and, as the name suggests, the basic idea is to focus in the image only the desired depth leaving the unwanted regions out of focus. This selective focusing can be obtained either by taking geometrical precautions while using analog detectors, such as screen-film cassettes, or by feeding the digital images to reconstruction algorithms to perform digitally the required operations[12]. In both planar and tomographic setting the rough description of the data acquisition process can be summarized as follows: First x-rays are somehow generated by the machine, the quality of these x-rays is optimized with the use of filters then focused and positioned such that they mostly hit the region that needs imaging. The beam then exits the machine and starts interacting with the imaged object[13], this process causes an attenuation in the beam which depends on the materials composing the object itself. Having then travelled across the whole object it interacts with a sensor, be it film, semiconductor or other, which stores the data that will then constitute the final image. In a digital setting this final step has to be performed following a (tomographic) reconstruction algorithm which given a set of 2D projections returns a single 3D image. In this light the interesting processes are how the radiation is created and shaped before hitting the patient and how said radiation then interacts with the matter of both the patient's body and the sensor beyond it. To explore these topics it's necessary to see:

- How these x-ray imaging machines are structured

[10] From the German terms *Bremsen* "to brake" and *Strahlung* "radiation"

[11] from the greek *Tomo* which means "to cut" and suffix -graphy to denote that it's a technique to produce images

[12] In the first case the process is referred to as *Geometric Tomography* while in the second case as *Digital Tomosynthesis*

[13] In this work it's always going to be a patient, however this process is general and is also used in industry to investigate object construction

- How x-ray and matter interact as the first traverses the second

It would also be interesting to talk about reconstruction algorithms however since it's beyond the scopes of this work MAGARI DIRE CHE USEREMO SOLO RICOSTRUZIONI DI UN TIPO QUINDI NON CI INTERESSA VEDERE LE DIFFERENZE?, refer to [13] and [30].

Generation and management of radiation: digital CT scanners

As of the writing of this thesis, seven generations of CT scanners with different technologies used. The conceptual structure of the machines is mostly the same, and the differences between generations also make evident those between machines. Exploiting this fact the structural description is going to be only one followed by a brief list of notable differences between generations.

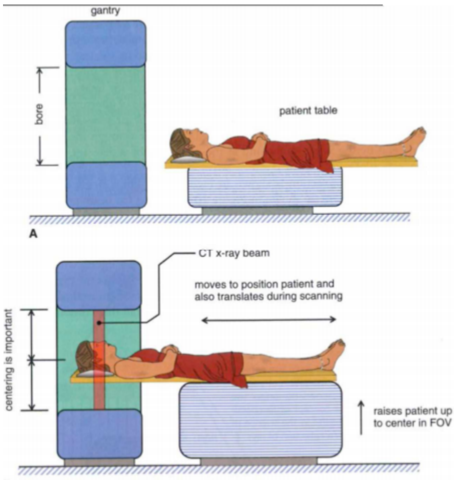
gantry
bore
patient table
A
CT x-ray beam
moves to position patient and also translates during scanning
centering is important
raises patient up to center in FOV

Figure 2.4: General set-up of a CT machine

The beam is generally created by the interaction of high energy particles with some kind of material, so that the particle's kinetic energy can be converted into radiation. In practice this means that an x-ray tube is encapsulated in the machine. Inside this vacuum tube charged particles[14] are emitted from the cathode, accelerated by a voltage differential and shot onto a solid anode[15]. This creation process implies that the spectrum of the produced x-rays is composed of the almost discrete peaks of characteristic emission, due to the atoms composing the target, superimposed with the continuum Bremsstrahlung radiation.

[14] Most commonly electrons

[15] Typical materials can be Tungsten, Molybdenum

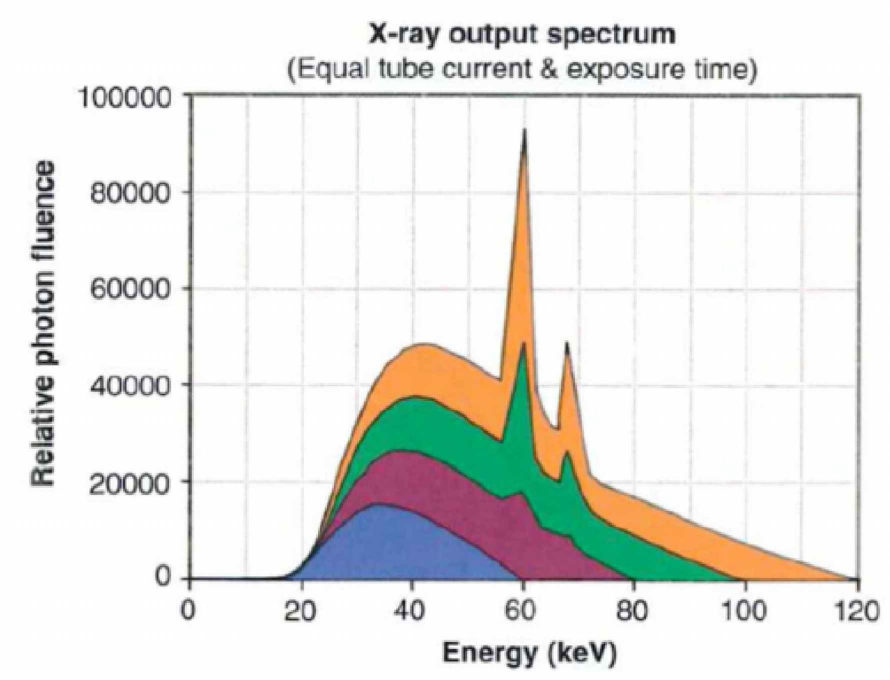

Figure 2.5: X-ray spectrum, composed of characteristic peaks and Bremsstrahlung continuum, computed at various tube voltages

Some of the main characteristics of the x-ray beam are related to this stage in the generation, the Energy of the beam is due to the accelerating voltage in the tube whereas the photon flux is determined by the electron current in the tube. Worth noting, en passant, that these two quantities can be found in the DICOM image of the exam as *kiloVolt Peak (kVP)* and *Tube current mA* and can be used to compute the dose delivered to the patient. Other relevant characteristics in the tube are the anode material, which changes the peaks in the x-ray spectrum and time duration of the emission, which is called exposure time and influences dose as well as exposure[16]. The electron energy is largely wasted ($\sim$ 99%) as heat in the anode, which then clearly needs to be refrigerated. The remaining energy, as said before, is converted into an x-ray beam which is directed onto the patient. To reduce damage delivered to the tissues it's important that most of the unnecessary photons are removed from the beam. Exploiting the phenomenon of beam hardening a filter, usually of the same material as the anode, is interposed between the beam and the patient to block lower energy photons from passing through thereby reducing the dose conveyed to the patient. At this point there may also be some form of collimation system which allows further shaping of the dose delivered. Having been collimated the beam traverses the patient and gets to the sensor of the machine, which nowadays are usually solid-state detectors. Naturally the description of these technologies can be done on a much finer level, however for the scopes of this work this description is deemed

[16] Exposure is a term used to identify how much light has gotten in the imaging sensor. Too high an exposure usually means the image is burnt, i.e. too bright and white, while lower exposures are usually associated to darker images. Exposure is proportional to the product of tube current and exposure time, measured in mA*s. Generally the machine handles the planning of exposure time according to treatment plan

sufficient FORSE ANCHE TROPPO? O TROPPO POCO?? At this point is where the differences between generations arise which,loosely speaking, can be found in the emission-detection configuration and technology.

- 1^{st} generation-Pencil Beam: A single beam is shot onto a single sensor, both sensor and beam are translated across the body of the patient and then rotated of some angle. The process is repeated for various angles. Main advantages are scattering rejection and no need for relative calibration, main disadvantage is time of the exam

- 2^{nd} generation-fan Beam: Following the same process as the previous generation the main advantage is the reduction of the time of acquisition by introducing N beam and N sensors which don't wholly cover the patient's body so still need to translate.

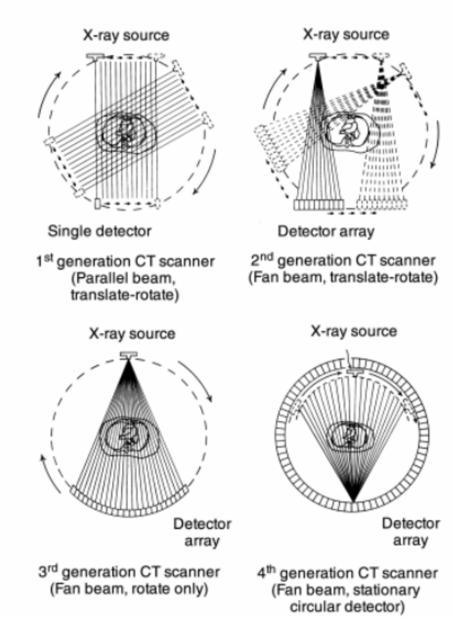
X-ray source
X-ray source
Single detector
Detector array
1st generation CT scanner (Parallel beam, translate-rotate)
2nd generation CT scanner (Fan beam, translate-rotate)
X-ray source
X-ray source
Detector array
Detector array
3rd generation CT scanner (Fan beam, rotate only)
4th generation CT scanner (Fan beam, stationary circular detector)

Figure 2.6: First four generation of CT scanners

- 3^{rd} generation-Rotate Rotate Geometry: Enlarging the span of the fan of beams and using a curved array of sensor a single emission of the N beams engulfs the whole body so the only motion necessary is rotation of the couple beam-sensor array around the patient.

- 4^{th} generation-Rotate Stationary Geometry: The sensors are now built to completely be around the patient so that only the beam generator has to rotate around the body

- 5^{th} generation-Stationary Stationary Geometry: The x-ray tube is now a large circle that is completely around the patient. This is only used in cardiac tomography and as such will not be described further [12]

- 6^{th} generation-Spiral CT: Supposing the patient is laying parallel to the axis of rotation, all previous generations acquired, along the height of the patient, a single slice at a time. In this generation as the tube rotates around the patients the bed on which they're laying moves along the rotation axis so that the acquisition is continuous and not start-and-stop. This further reduces the acquisition time while significantly complicating the mathematical aspect of the reconstruction. It's necessary to add another important parameter which is the pitch of the detector[17]. This quantifies how much the bed moves along the axis at each turn the tube makes around the patient. Pitches smaller than one indicate oversampling at the cost of longer acquisition times, pitches greater than one indicate shorter acquisition times at the expense of a sparser depth resolution.

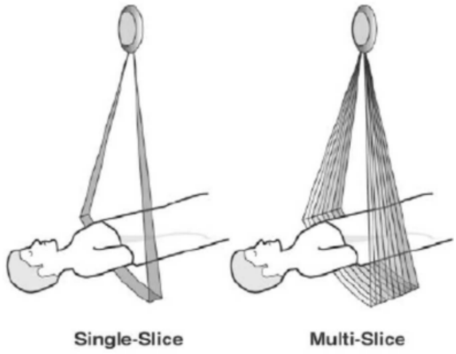

Figure 2.7: $7^{th} generationsetup$

- 7^{th} generation-MultiSlice: Up to this seventh generation height-wise slice acquisition was of a singular plane, be it continuous or in a start and stop motion. In this final generation mutliple slices are acquired. Considering cilindrical coordinates with z along the axis of the machine the multiple slice acquisition is obtained by pairing a fanning out along θ and one along z of both sensor arrays and beam. This technique returns to a start and stop technology in which only $\sim 50\%$ of the total scan time is used for acquisition

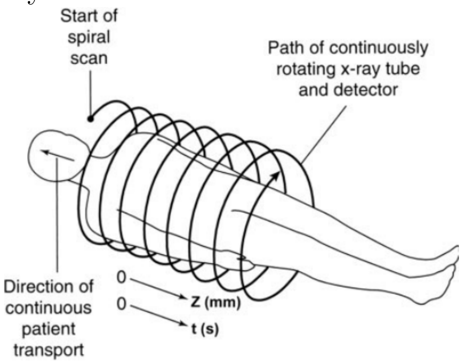
Start of spiral scan
Path of continuously rotating x-ray tube and detector
Direction of continuous patient transport
0
0
Z (mm)
t (s)

Figure 2.8: $7^{th} generationsetup$

The machines used to obtain the images used in this thesis, all belonging to the Ospedale S. Orsola, were distributed as follows shown in 2.9:

[17] Once again the important parameters, such as this, can be accessed in the DICOM file resulting from the exam,

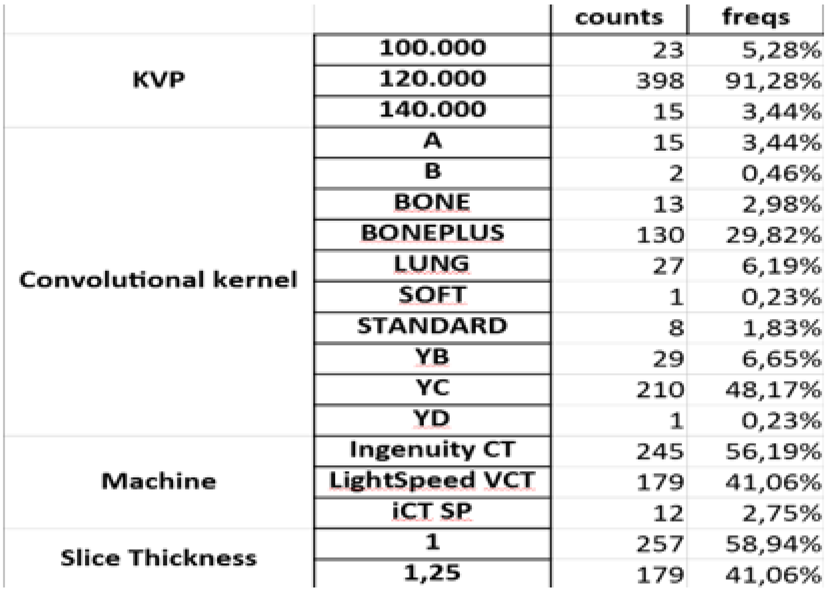

		counts	freqs
KVP	100.000	23	5,28%
	120.000	398	91,28%
	140.000	15	3,44%
Convolutional kernel	A	15	3,44%
	B	2	0,46%
	BONE	13	2,98%
	BONEPLUS	130	29,82%
	LUNG	27	6,19%
	SOFT	1	0,23%
	STANDARD	8	1,83%
	YB	29	6,65%
	YC	210	48,17%
	YD	1	0,23%
Machine	Ingenuity CT	245	56,19%
	LightSpeed VCT	179	41,06%
	iCT SP	12	2,75%
Slice Thickness	1	257	58,94%
	1,25	179	41,06%

Figure 2.9: Acquisition parameter and machine distribution

1. Ingenuity CT (Philips Medical Systems Cleveland): $\sim 56\%$ of the exams were obtained with this machine

2. Lightspeed VCT (General Electric Healthcare, Chicago-Illinois): $\sim 41\%$ of the exams in study come from this machine

3. ICT SP (Philips Medical Systems Cleveland): $\sim 3\%$ of the exams were performed with this machine

Radiation-matter interaction: Attenuation in body and measurement

Having seen the apparatus for data collection the remaining task is to see how the information regarding the body composition can be actually conveyed by photons. Let's first consider how a monochromatic beam of x-rays would interact with an object while passing through it. All materials can be characterized by a quantity called attenuation coefficient μ which quantifies how waves are attenuated traversing them, this energy dependent quantity is used in the Beer-Lambert law which allows computation of the surviving number of photons, given their starting number N_0 and μ:

$$N(x) = N_0 e^{-\mu(E)*x} \tag{2.3}$$

At a microscopic level the absorption coefficient will depend on the probability that a photon of a given energy E interacts with a single atom of material. This can be expressed using atomic cross section σ as:

$$\mu(E) = \frac{\rho * N_A}{A} * (\sigma_{Photoelectric}(E) + \sigma_{Compton}(E) + \sigma_{PairProduction}(E)) \qquad (2.4)$$

Where ρ is material density, N_A is Avogadro's number, A is the atomic weight in grams and the distinction among the various possible interaction processes for a generic photon of high energy E is made explicit. Overall the behaviour of the cross section is the following

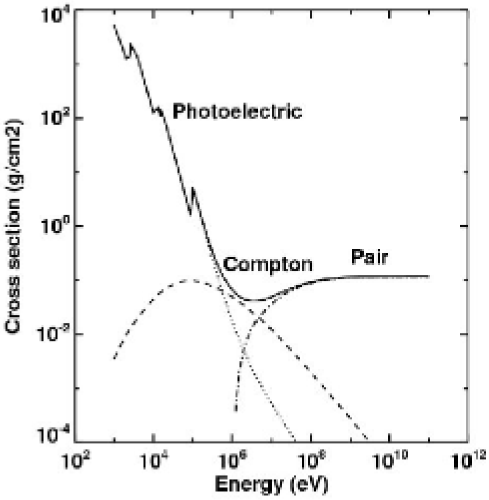

Figure 2.10: Photon cross-section in Pb

Overall, given eq:2.3, it's clear to see that the attenuation behaviour of a monochromatic beam would be linear in semi-logarithmic scale hence the name for μ "*Linear Attenuation Coefficient*". The first complication comes from the fact that, given their generation method, the x-rays are not monochromatic but rather polychromatic. This introduces a further complication which is the phenomenon of beam hardening: lower energy x-rays interact much more likely than those at higher energies which implies that as it crosses some material the mean energy of the whole beam increases. This behaviour is exploited still within the machine, filters are interposed between anode and patient to reduce the useless part of the spectrum as shown in fig: 2.11a:

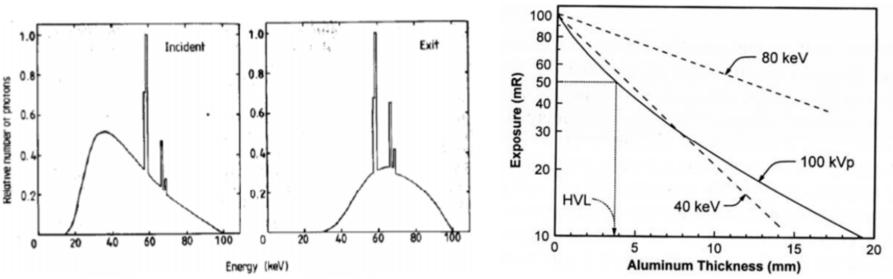

(a) Beam Filtering

(b) Polychromatic beam attenuation

Figure 2.11: Polychromatic beam behaviour

Another effect of the beam being polychromatic is that the graphical behaviour of the attenuation instead of being linear gets bent as shown in fig: 2.11b. Since the image brightness is related to the number of photons that get on the sensor it's still possible to define the contrast between two pixel p_1, p_2 as:

$$C(p_1, p_2) = \frac{N_{\gamma,p_2} - N_{\gamma,p_1}}{N_{\gamma,p_2}} \tag{2.5}$$

This formula, that connects the beam to the image, together with eq: 2.3, which connects the beam property to the patient's composition, make clear the processes by which the beam carries patient information. Another complication arises in the context of this last equation due to the phenomenon of scattering which reduces the contrast by changing the direction of the bean and introducing an element of noise. Anti-scattering grids are positioned right before the sensors to reduce this effect by allowing to reach the sensor to only the photons with the correct direction.
The biological effects of radiation won't be treated in this thesis. Suffices to say that damage can be classified as primary, due to ionization events within the nucleus of the cell, or secondary, due to chemical changes in the cell environment. The energy deposited per unit mass is called dose and is measured in Gy(Gray) and, as said before, depends on exposure time, current and kVP of the tube. Most of contemporary machines for CT self-regulate exposure time during the acquisition automatically using Automatic Exposure Control(AEC). Having the dose it's possible to estimate the fraction of surviving cells and, to do so, various models are used. In the clinical practice it's common to find, still within the DICOM image metadata, the information regarding Dose delivered such as CTDI (Computed Tomography Dose Index) from which it's possible to obtain the DLP (Dose Length Product) taking into consideration the total length of irradiated body. For an introduction to one of these models, the Linear Quadratic (LQ) refer to [20].

2.1.2 Artificial Intelligence (AI) and Machine Learning(ML)

Having clarified the type of data that will be used in this work, and having seen the general procedure used to gather it, it becomes interesting to discuss what kind of techniques will be used to analyze it. Starting from the definition given by John McCarthy in [18] "[AI] is the science and engineering of making intelligent machines, especially intelligent computer programs. It is related to the similar task of using computers to understand human intelligence, but AI does not have to confine itself to methods that are biologically observable.". Machine Learning (ML) is a sub-branch of AI and contains all techniques that make the computer improve performances via experience in the form of exposure to data, practically speaking this finds it's application in classification problems, image/speech/pattern recognition, clustering, autoencoding and others. The general workflow of Machine Learning is the following: given a dataset, the objective is to define a model or function which depends on some parameters which is able to manipulate the data in order to obtain as output something that can be evaluated via a predefined performance metric. The parameters of the model are then automatically adjusted in steps to minimize or maximize this performance metric until a stable point at which the model with the current parameters is considered finalized; one of the main problems in this procedure is being sure that the stable point found is global and not local. MAGARI FORSE POTREBBE ESSERE CARINO SPIEGARE UN PO' DI DISCESA DEL GRADIENTE. The whole procedure is carried out keeping in mind that the resulting model needs to be able to generalize it's performance on data that it has never seen before, for this reason usually ML is divided in a training phase and a testing phase. The training phase involves looking at the data and improving the performance of the model on a specific dataset[18], the testing phase involves using brand new data to evaluate the performance of the model obtained in the preceding phase. Machine Learning techniques can be further grouped into the following categories:

1. Supervised Learning: In this type of ML the model is provided with the input data as well as the correct expected output, which is hence called *label*. The objective of the model is to obtain an output as similar to the labels as possible, while also retaining the best possible generalization ability in predicting never seen before data. Some problems that benefit from the use of these techniques are regression and classification problems.

2. Unsupervised Learning: As the name suggests this category of models trains on the data alone, without having the labels available by minimizing some metric defined from the data. For example clustering techniques try to find a set of groups in the data such that the difference within each group is minimal while

[18] Usually in studies there is a single dataset which is split into a train-set and a test-set, in some cases if the model is good it can be validated prospectively, which means that it's performance is evaluated on data that did not yet exist at the time of birth of the model

the difference among groups is maximal, ideally producing dense groups, called clusters, that are each well separated from all the others. Other techniques in this family are Principal Component Analysis (PCA) and autoencoding but the general objective is to infer some kind of structure within the data and the relation between data points.

3. Reinforcement Learning: This kind of ML is well suited for data which has a clear sequential structure in which the requiered task is to develop good long term planning. Broadly speaking the general set-up is that given a set of (state$_t$, action, reward, state$_{t+1}$) these techniques try to maximize the cumulative reward[19]. The main applications of these techniques are in Autonomous driving and learning how to play games

The following methods are those directly involved in this work.

Regression, Classification and Penalization

Regression and Classification are methods used to make predictions via supervised learning by understanding the input-output relation in continuous and discrete cases respectively. The most basic example of regression is linear regression which consists in finding the slope and intercept of a line passing through a set of points. A branch of classification thats similar to linear regression is logistic regression, this translates in finding out wether or not each point belongs to a certain category given it's properties and can be practically thought of, for a binary classification,as a fitting procedure such that the output can be either 0 for one category and 1 for the other, this is usually done using the logistic funtion, also called sigmoid, which compresses $\mathbb{R}$ in [0,L] as seen in 2.12. L represents the maximum value desidered, x_0 is the midpoint and k is the steepness. Note that for multiple categories it would conceptually suffice to add sigmoids with different centers to obtain a step function in which each step corresponds to a category, in this case the procedure is usually called multinomial regression.

$$\sigma_{(x)} = \frac{L}{1 + e^{-k(x - x_0)}} \tag{2.6}$$

[19] i.e. the sum of the rewards obtained at all previous time steps

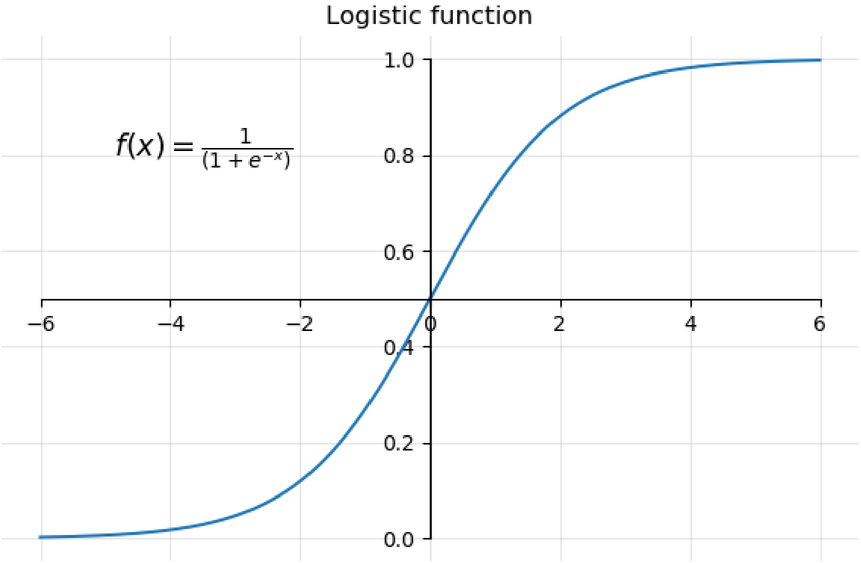

Figure 2.12: sigmoid function with L=1, x_0=0, k=1

To give a general intuition of the procedure, without going in unnecessary details, let's only consider linear regression; the theory on which it is founded is based on the assumption that the residuals, i.e. the distance model-label, are normally distributed. Under this assumption the parameters can be found by changing them and trying to minimize the sum of squared residuals. When each datapoint is characterized by a lot of different features the procedure is called multiple linear regression, the task becomes finding out how much each feature contributes in predicting the output within a weighted linear combinaion of features. Practically speaking this can be done in matricial form, supposing that each of the m datapoints has n features associated let **X** be a matrix with n+1[20] columns and m rows and let **Y** be a vector with m entries. Let also θ be a vector of n+1 entries, one for each feature plus the intercept θ_0, then we are supposing that:

$$y_i = \Sigma_{j=0}^{n+1} x_{i,j} * \theta_i + \epsilon_i => \mathbf{Y} = X * \theta + \epsilon \tag{2.7}$$

Where ϵ is the array of residuals of the model which, as said before, is supposed to contain values that are normally distributed. Minimizing the squared residuals corresponds to minimizing the following cost function:

$$J_\theta = (\mathbf{Y} - X * \theta)^T * (\mathbf{Y} - X * \theta) \tag{2.8}$$

By setting $\frac{\delta J}{\delta \theta}$=0 it can be shown that the best parameters θ^* are :

[20] n+1 because we have n features but we also want to estimate the intercept of the line, so in practice the first column will be of all ones to have the correct model shape in the following matrix multiplication

$$\theta^* = (\mathbf{X}^T * \mathbf{X})^{-1} * \mathbf{X}^T\mathbf{Y} \tag{2.9}$$

It's evident that to obtain a result from the previous operation it's necessary that $(\mathbf{X}^T * \mathbf{X})$ be invertible, which in turn requires that there be no correlated features and that the features be less than the datapoints. To solve this problem the first step is being careful in choosing the data that goes through the regression, which may even involve some preprocessing. The second step is called Regularization, it involves adding a penalty to the cost function by adding a small quantity along the diagonal of the matrix. The nature of this small quantity changes the properties of the regularization procedure, the most famous penalties are Lasso, Ridge and ElasticNet. In practical terms the shape of the penalty determines how much and how fast the slopes relative to the features can be shrunk.

1. Ridge: Adds $\delta^2 * \Sigma_{j=1}^{n+1}\theta_j^2$, is called also L^2 regularization since it adds the L^2 norm of the parameter vector. This penalty can only shrink parameters asymptotically to zero but never exactly, which means that all features will always be used, even with very small contributions
2. Lasso: Adds $\frac{1}{b} * \Sigma_{j=1}^{n+1}|\theta_j|$, is called also L^1 regularization since it adds the L^1 norm of the parameter vector. This penalty can shrink parameters to exactly zero, getting rid of the useless variables within the model.
3. ElasticNet: Adds $\lambda * [\frac{1-\alpha}{2} * \Sigma_{j=1}^{n+1}\theta_j^2 + \alpha * \Sigma_{j=1}^{n+1}|\theta_j|]$, evidently this is a midway between the Lasso and Ridge methods, where the balance is dictated by the value of α.

Following regularization procedures, specifically Lasso regularization, as a byproduct of avoiding divergences a selection and ranking of the important features is obtained however it's still important to preprocess the data to simplify the job of the regularization.

forse questo è meglio in materiali e metodi?

Since the whole foundation is the normality of the residuals it's important that the data behaves somewhat nicely in this regard. Changing the data to modify the residuals is not straightforward, a proxy for this procedure is to preprocess the data by manipulating the distribution of the features to make them as close to normal as possible. To this end some of the operations that can be done are:

1. Standard Scaling: This amounts to subtracting the mean of the distribution to the feature and dividing by the standard deviation so that the resulting distribution is somewhat centered around zero and has close to unitary standard deviation

2. Boxcox transform: When distributions are heavy-tailed, like a gamma distribution would be, this finds the best exponent to transform via a power-law the data. Since the exponent $\lambda \in \mathbb{R}$ the input data needs to be strictly positive and not constant.

Practical application of these procedures can be found in cap:2. These considerations conclude the theoretical background on regression, classification and penalization thereof.

Decision Trees and Random Forest

Apart from logistic and multinomial regression there are various other supervised classifiying methods such as Support Vector Machines (SVM), Neural Networks and Decision Trees. In this thesis, among the aforementioned algorithms, the chosen one was a particular evolution of DecisionTrees called RandomForest (RF). To provide some insight in the method it's necessary to first explain how decision trees work, specifying what problems they face and what are their strong points. Since it's a classification method let's consider the simple case of binary classification with categorical[21] features. The task of the decision tree is to approximate to the best of it's abilities the labels contained in the training set using all the features associated with each datapoint, this is done by building a graph-like structure in which the nodes represent the features and the links departing from it are the possible values the feature takes. This graph is built in a top-down approach by choosing at every step the feature that best separates the data in the label categories, this process is done along each branch unitl a node in which the separation of the preceding feature is better then that provided by all remaining features or all features have been considered. The first node is called root node, while the nodes that have no branches going out of them are called leaves, the graph represents a tree hence the name of the method. Note that at every node only the subset of data corresponding to all previous feature categories is used. At each node the separation between the two label categories c_1, c_2 due to the feature is commonly measured with Gini

[21] Categorical is to be intended as features with discrete value, opposed to continuous variables which can potentially take any value in $\mathbb{R}$

impurity coefficient, which is computed as:

$$\begin{aligned} G &= 1 - p_1^2 - p_2^2 \\ &= 1 - \left[\frac{N_{c_1 \in node}}{N_{samples \in node}}\right]^2 - \left[\frac{N_{c_2 \in node}}{N_{samples \in node}}\right]^2 \end{aligned} \tag{2.10}$$

The Gini impurity for a feature is then computed as an average of the gini coefficients of all the deriving nodes weighted by the number of samples in each of the nodes. This method can be obviously generalized to cases in which features are continuous by thresholding the features choosing the value that best improves the separation of the deriving node, a way to choose possible thresholds is to take all the means computed with all adjacent measurements. It's important to note firstly that there is no restiction on using, along different branches, different tresholds for the same feature and, secondly, that the same featue can end up at different depths along diffenrent branches. The strength of this method is it's performance on data it has seen however it has very poor generalization abilities, Volendo si può citare elements of statistical learning

Random Forests algorithms are born to overcome this problem. As the name suggests the idea is to build an ensemble of Decision Trees in which the features used in the nodes are chosen among random subsamples of all the available features, the final result is obtained as a majority vote over all trained trees. Each tree is also trained on a bootstapped dataset created from the original, this procedure might exacerbate some problems of the starting dataset by changing the relative frequency of classes seen by each tree and can be corrected by balancing the bootstrap procedure. This method vastly improves the performance and robustness of the final prediction while retaining the simplicity and ease of interpretation of the decision trees, naturally there are methods, such as AdaBoost, to deploy and precautions, such as having balanced dataset, to take to further improve the performance of RF classifiers. In the context of this thesis it will become necessary to take care of balancing the input dataset, to do so one could randomly oversample, by duplicating instances in the minority class, or undersample, by removing instances within the majority class. The choice that was made was to use Synthetic Minority Oversampling TEchnique (SMOTE)[6] to rebalance the dataset.

Synthetic Minority Oversampling TEchnique (SMOTE)

This technique considers a user-defined number of nearest neighbours of randomly chosen points in the minority class and populates the feature space by generating samples on the lines that connect the chosen sample with a random neighbour[22].

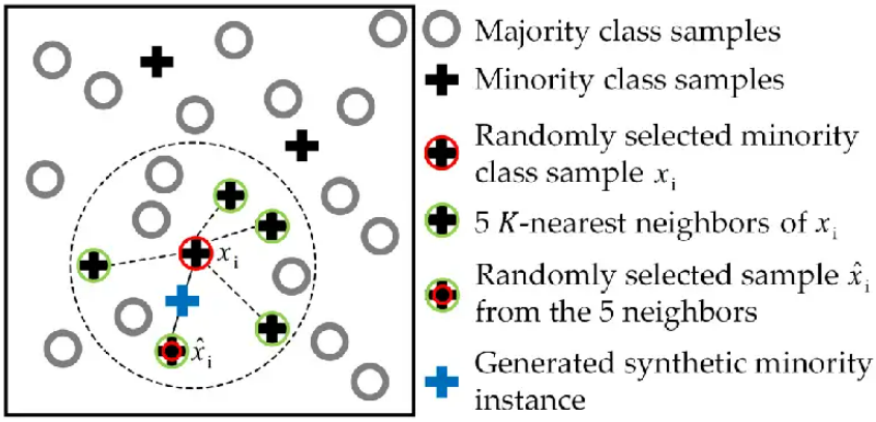
x_i
$\hat{x}_i$
Majority class samples
Minority class samples
Randomly selected minority class sample x_i
5 K-nearest neighbors of x_i
Randomly selected sample $\hat{x}_i$ from the 5 neighbors
Generated synthetic minority instance

Figure 2.13: Example of SMOTE with 5 nearest neighbours

Worth noting that this has been done using the library imblearn in python [17]. To preview some of the data, looking at the performance of a vanilla random forest implementation with all preset parameters, the effect of the position of oversamplling is the following.

[22] This procedure is formally called convex combination, which is a peculiar linear combination of vector in which the coefficients sum to one. Particularly all convex combination of two points lay on the line that connects them, and for three point lay within the triangle that has them as vertices

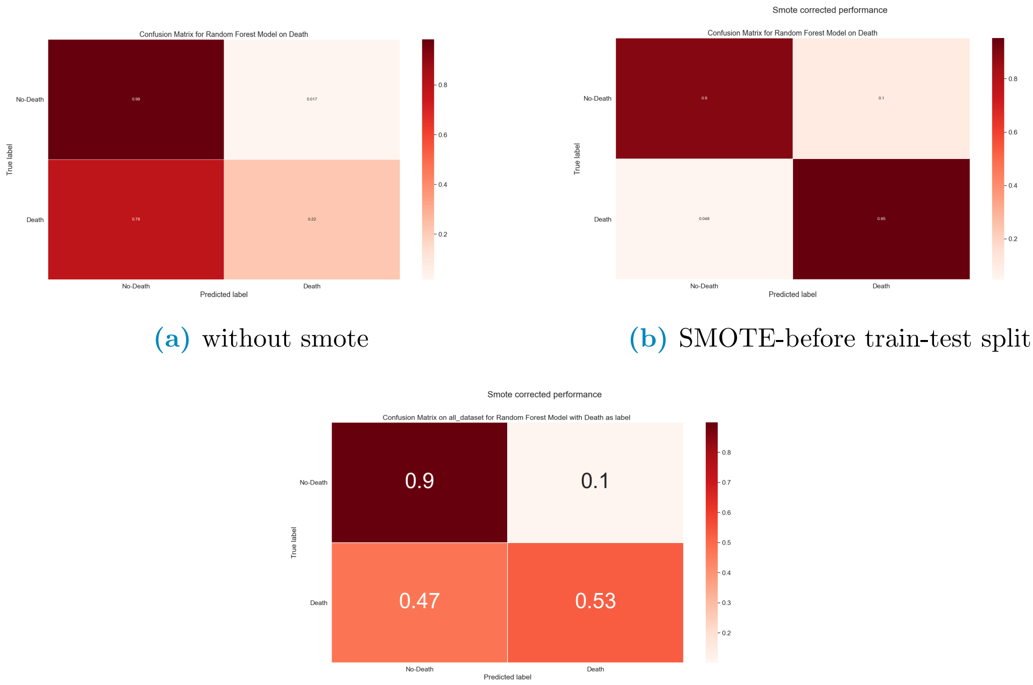

(a) without smote

(b) SMOTE-before train-test split

(c) SMOTE after train-test split

Figure 2.14: Confusion matrix used to evaluate performance done using datasets with various combinations of SMOTE position

It's clear to see that in unbalanced case, like the one analysed in this thesis in which the label classes are 15%-85%, oversampling the data always determines an improvement in performance. However performing it in the wrong place it clearly makes a far too optimistic evaluation of the performance. This highlights the point that all preprocessing should be done with care when train-test splitting the data, specifically it's very important that the oversampling, as well as all other data handling, be performed after the train-test split of the data on the train data alone. It's clear to see that what's being observed is a leakage phenomenon, in which the testing data contiains information regarding the training data and viceversa. In practice, especially because the points are created as convex combination of existing data[23], when the synthetically generated points end up in the testing they depend, at least partially, on the data used in the training procedure.

[23] Note that this would happen with any other over/under-sampling methods, such as random oversampling which randomly duplicates data points

Dimensionality reduction and clustering

When dataset are composed of many features, namely more than three, it becomes difficult if not impossible to visualize the distribution of data. There are various techniques that can mitigate or solve this problem, they are grouped under the umbrella term of "Dimensionality reduction techniques" and they are generally based on ML learning methods. As such , following the same reasoning and definitions given in regard to ML, it's possible to introduce a sub-categorization of the whole family of techniques in supervised and unsupervised techniques. Dimensionality reduction, beyond providing useful insight in the general structure of the data, can also be used as a preprocessing step in some analysis pipelines. A first example could be to find more meaningful features before analyzing with methods such as Random Forests or Regression techniques, a second example could be using the reduced representation that keeps the most information possible to ease in clustering analysis by highlighting the differences in subgroups within the dataset. The most common dimensionality reduction techniques are:

1. **Unsupervised methods**

   - Principal Component Analysis (PCA): Linearly combines the pre-existing features to obtain new ones and orders them by decreasing ability to explain total variance of data. The first principal component is the combination of features that most explains the variance in the original dataset. Given it's nature it focuses on the global characteristics of the dataset.
   - t-distributed Stochastic Neighbor Embedding (t-SNE): Keeps a mixture of local and global information by using a distance metric in the full high dimensional space and trying to reproduce the distances measured in the lower dimensional space which can be 2- or 3-dimensional. NON SO SE VA SPIEGATO MEGLIO O PIU' IN DETTAGLIO
     Let's define similarity between two points as the value taken by a normal distribution in a point away from the centre, corresponding to the first point of interest, the same distance as the two points taken in consideration. Fixing the first point the similarities with all other points can be computed and

normalized. Doing this procedure for all points it's poissible to build a normalized similarity matrix. Then the whole dataset is projected in the desired space, usually $\mathbb{R}^i$ with i=1,2 or 3, in which a second similarity matrix is built using a t-distribution instead of a normal distribution [24]. At this point, in iterative manner, the points are moved in small steps in directions such that the second matrix becomes more similar to the one computed in the full space.

2. **Supervised methods**

   - Partial Least Squared Discriminant Analysis (PLS-DA): This technique is the classification version of Partial Least Squares (PLS) regression. Much like PCA the idea is to find a set of orthonormal vectors as linear combination of the original features in the dataset, however in PLS and PLS-DA is necessary to add the constraint that the new component, besides being perpendicular to all previous ones, explains the most variability in a given target variable, or set thereof. For an in depth description refer to [4] while for a more modern review refer to [16] Hanno senso queste due in bibliografia?

3. **Mixed techniques**

   - Uniform Manifold Approximation and Projection (UMAP): Builds a network using a variable distance definition on the manifold on which the data is distributed then uses cross-entropy as a metric to reproduce a network with the same structure in the space with lower dimension. This technique maintains very local information on the data and allows a complete freedom in the choice of the final embedding space as well as the definition of distance metrics in the feature space[25], it's also implemented to work an a generic pandas dataframe in python so it can take in input a vast range of datatypes. The math behind this method is much beyond the

[24] The use of this t-distribution gives the name to the technique, the need for this choice is to avoid all the points bunching up in the middle of the projection space since t-distributions have lower peaks and are more spread out than normal distributions. For more details refer to [**?**]

[25] Actually to keep the speed in performance the distance function needs to be Numba-jet compilable

scopes of this thesis, as such refer to [19] for more in depth information.

It should be noted that dimensionality reduction is not to be taken as a necessary step, however it can reduce the noise in the data by extrapolating the most informative features while easing in visualization and reducing computational costs of subsequent data analysis. These upsides become particularly relevant in the field of clustering, where the objective is to group data in sets with similar features by minimizing the differences within each group while maximizing the differences between different groups. Clustering techniques can be roughly divided in:

1. Centroid based techniques: A user defined number of points is randomly located in the data space, datapoints are then assigned to groups according to their distance from the closest center. The main technique in this category is k-means clustering, and some, if not most, other techniques include it as step in the processing pipeline[26]. The main problems are firstly that these techniques require prior knowledge, or at the very least a good intuition, on the number of clusters in the dataset while also assuming that the clusters are distributed in spherical gaussian distribution, which is not always the case.

2. Hierarchical clustering: The idea is to find the hierarchical structure in the data using a bottom-up or a top-down approach, as such this category further subdivides in agglomerative and divisive methods. In the first each point starts by itself and then points are agglomerated using a similarity or distance metric, this build a dendrogram in which the kth level roughly corresponds to a k-centrouid clustering. In the latter the idea is to start with a unique category and then divide it in subgroups.

3. Density based techniques: These methods use data density to define the groups by looking for regions with larger and lower density as clusters and separations.

[26] An example of such techniques is: affinity propagation

In order to evaluate the performance of these methods it's necessary to define metrics that evaluate uniformity within clusters and separation among them, the choice in the definition of metric should be taken in careful consideration since the different task may imply very different optimal metrics or, put differently, the optimal technique for the task at hand may very well depend on the metric used. It's worth mentioning that when working in two, or at most three, dimensions humans are generally good at preforming clustering yet it's nearly impossible to do in more dimensions. Computers, on the other hand, require more careful planning even in low dimension but are much more performing even in higher dimensions because the generally good human intuition on the definition of cluster is not so easily translated in instruction to a machine. So to obtain good results with clustering techniques it necessary to work with care, expecially with a good understanding of the dataset in use and it's overall structure. In the context of this thesis, supposing the data suggested a clear cut distinction of two populations in the dataset, as could be male-females or under- vs normal- vs over-weight individuals, then it might become necessary to analyse these groups as different cohorts in order to more accurately predict their clinical outcome.

2.1.3 Combining radiological images with AI: Image segmentation and Radiomics

Having seen the kind of data that will be of interest throughout this thesis, and having a set of techniques used describe and make predicition on the data at hand, the final step in this theoretical background chapter will be to combine these two notion in describing first how images can be treated in general terms and then, more specifically, how medical images can be analysed to exploit as much as possible the vast range of information they contain. Image analysis seems, at first glance, very intuitive since for humans it's very easy to infer qualitative information from images. However upon closer inspection this matter becomes clearly non trivial due to the subjectivity involved in the process as well as in the intuition behind it. More specifically, in the context of this thesis, the same image of damaged lungs contains very different informations to the eyes of trained professional versus those of an ordinary person as well as to the eyes of different professionals. The first big obstacle in this task is the definition of region of interest: not all people will see the same boundary in a damaged organ, sometimes the process of defining a boundary between organ and tissue may need to account for the final objective it has to achieve. If the objective is to evaluate texture of a damaged lung then the lesion needs to be included whereas in other cases these regions may only be unwanted noise. Generally speaking finding regions of interest in an image is a process called image segmmentation. The next step would be to quantify the characteristics of the region identified, as such it should be clear that finding ways to derive objective information from images it's of paramount importance, expecially when this information can aid in describing the health of a patient. It should also be clear that medical images are a kind of high dimensional data as such, as it's fashion with fields that occpy themselves with big biological data, the field that studies driving quantitative information out of radiological images is called radiomics.

Image Segmentation

Generally speaking image segmentation is a procedure in which an image is divided in smaller sets of pixels, such that all pixel inside a certain set have some common property and such that there are no overlaps between sets. These sets can then be used for further analysis which could mean foreground-backgroud distinction, edge detection as well as object detection, computer vision and pattern recognition. Image segmentation can be classified as:

- Manual segmentation: The regions of interest are manually defined usually by a trained individual. The main advantage of this it's the versatility, on the other hand this process can be very time consuming

- Semi-automatic segmentation: A machine defines as best as it can the shape of the region of interest, however the process is then thought to receive intervention of an expert to correct the eventual mistakes or refine the necessary details. This provides the best compromise between time needed and accuracy obtained and becomes of interest in fields in which finer details are important.

- Automatic segmentation: A machine performs the whole segmentation without requiring human intervention

On a practical level these techniques can be used in various fields, as illustrated by the variety of aforementioned tasks, but the one that interests this work the most is the medical field. Nowadays in medicine, where most of imaging exams are stored in digital form, the ability to automatically discern specific structures within the images can provide a way to aid clinical professionals in their everyday decision making their workload lighter and helping in otherwise difficult cases. A staggering example connected to this thesis is the process of organ segmentation in CT scans: usually these scans are n[27] stacked images in 512x512 resolution. To have a contour of the lungs in a chest CT a radiologist would need to draw by hand the contour of the lung in each slice of the scan. Even if some shorcuts exist to reduce the number of slices to draw on this very boring, time consuming and repetitive task can occupy hours if not days of work to a human while a machine can take minutes to complete a whole scan. Then considering lesion detection in medical exams having a machine that consistently finds lesions that would otherwise be difficult to discern by a human eye can be of paramount importance in diagnosis as well as treatment. In the medical field the difficulty comes from the fact that different exams have different types of image formats which means that an algorithm that works well on CT may not work as intended on MRI or other procedures. Automatic image segmentation can be performed in various ways:

1. Artificial Neural Network (ANN): These techniques belong to a sub-field in ML called Deep Learning, they involve building network structures with more layers in which each node is a processing unit that takes a combination of the input data and gives an output according to a certain activation function. These structures are called Neural Networks because they resemble and are

[27] n clearly depends on the exam required and slice thickness, some common values for thoracic CTs are around 200-300 but can range up to 900 slices

modeled after the workings of neuron-dendrite structures while the deep in deep learning refers to the fact that various layers composed of various neurons are stacked one after the other to complete the structure. Learning is obtained by changing how each neuron combines the inputs it recieves. In the case of images these structures are called Convolutional Neural Networks because the first layers, which are intended to extract the latent features or structures in the images, perform convolution operation in which the parameters are the values pixel values of convolutional kernels

2. Thresholding: These techinques involve using the histogram of the image to identify two or more groups of pixel values that correspond to specific parts/objects within the image. An obvious case would be a bi-modal distribution in which the two sets can be clearly identified but there are no requirements on the histogram shape. In the case of CT this has a very simple and clear interpretation since HU depend on tissue type it's reasonable to expect that some tissues can be differentiated with good approximation by pixel value alone

3. Deformable models and Region Growing: Both these technique involve setting a starting seed within the image, in the first case the seed is a closed surface which is deformed by forces bound to the region of interest, such as the desired edge. In the second case the seed is a single point within the region of interest, step by step more points are added to a set which started as the seed alone according to a similarity rule or a predefined criteria.

4. Atlas-guided: By collecting and summarizing the properties of the object that needs to be segmented it's possible to compare the image at hand with these properties to identify the object within the image itself.

5. Classifiers: These are supervised methods that focus on classifying via by focusing on a feature space of the image. A feature space can be obtained by applying a function to the image, an example of feature space could be the histogram. The main distinction from other methods is the supervised approach

6. Custering: Having a starting set of random clusters the procedure computes the centroids of these clusters, assigns each point to the closest cluster and recomputes centroids. This is done iteratively until either the point distribution or the centroid position doesn't change significantly between iterations.

For a more in depth review of the main methods used in medical image segmentation refer to [24]. Worth noting, at this point, that the semi-automatic segmentation software used in this work uses probably a mixture of region growing and thresholding methods, maybe guided by an atlas. The segmentation process generally produces a boolean mask which can be used to select, using pixel-wise multiplication, the region of interest in the image. The next step in image analysis would be to derive information from the region defined during segmentation, in general this step is called feature extraction[28] and it's objective is to find non-redundant quantities that meaningfully summarize as much properties of the original data as possible.

Radiomics

When the images are medical in nature and when referring to high-throughput quantitative analysis the task of finding these features fall in the realm of radiomics, which uses mathematical tools to describe properties of the images that would otherwise be unquantifiable to the human eye. The features that can be computed from images are of various types, some of them can be understood somewhat easily through intuition since they are close to what humans generally use to describe images, others are much more complex in definition and quantify more difficulty percieved properties of the image. Features can be then roughly classified in different families:

1. Morphological features: These features describe only the shape of the region of interest, as such they are independent of the pixel values inside the region and hence, to be computed, require only a boolean mask of the segmented region. These features can be

[28] Even if the term is used in pattern recognition as well as machine learning in general

further subcategorized as two or three dimensional features based on whether they focus on single slices or whole volumes. Most of these features compute volumes, lengths, surfaces and shape properties such as sphericity, compactness, flatness and so on.

2. First order features: These features depend strictly on the gray levels within the region of interest since they evaluate the distribution of these values, as such they need that the boolean mask of the segmentation be multiplied pixel-wise with the origian image to obtain a new image with only the interesting part in it. Most of these features are commonly used quantities, such as Energy, Entropy, Minimum and Maximum value which have been adapted to the imaging context using the histogram of the original image or by considering intensities within an enclosed region.

3. Higher order features: All the other fatures fall in this macro-category which can be clearly subdivided in other smaller catgories in which the features are obtained following the same guiding principle or starting point. Generally these describe more texture-like properties of the image and, to do so, use particular matrices derived from the original image which contain specific information regarding order and relationships in pixel value positioning within the image. These matrices have very precise definition, as such only the general idea behind them will be reported here redirecting to [32] for a more strict and in detail description. The matrices from which the features are computed also give name to the smaller categories in this family, these categories are:

    - Gray Level Co-occurence Matrix (GLCM) features: This matrix expresses how combination of pixel values are distributed in a 2D or 3D region by considering connected all neighbouring pixel in a certain direction with respects to the one in consideration. Using all possible directions for a set distance, usually δ=1 or δ=2, various matrices are obtained and from these a probability distribution can be built and evaluated. It should be noted that before computing these matrices the intensities in the image are discretized.
    - Gray Level Run Length Matrix (GLRLM) features: Much like before the task of these features is to quantify the distri-

bution of relative values in gray levels trhoughout the image, as the name suggests what this matrix quantifies is how long a path can be built by connecting pixel of the same value along a single direction. This time information from the matrices computed by considering different directions are aggregated in different ways to improve rotational invariance of the final features

- Gray Level Size Zone Matrix (GLSZM) features: This matrix counts the number of zones in which voxel have the same discretized gray level. The zones are defined by a notion of connectedness most commonly first neighbouring voxel are considered as connectable if they have the same value, this leads to a 26 neighbouring voxel in 3 dimensions and to 8 connected pixels in 2 dimensions[29]. The matrix contains in position (i,j) the number of zones of size j in which pixel have value i.
- Neighbouring Gray Tone Difference Matrix (NGTDM) features: Born as an alternative to GLCM these features rely on a matrix that contains the sum of differences between all pixel with a given pixel value and the average of the gray levels in a neighbourhood around them.
- Gray Level Dependence Matrix (GLDM) features: The aim of these features is to capture in a rotationally invariant way the texture and coarsness of the image. This matrix requires the already seen concept of connectedness with a given distance as well as dependence among pixel. Two voxel in a neighbourhood are dependent if the absolute value of the difference between their discretized value is less then a certain threshold. The number of dependent voxel is then counted with a particular approach to guarantee that the value be at least one

In talking about the previous feature groups the concept of discretization of data which is already digital, and hence a discretized, has emerged. This is often a required step to make the computations

[29] To visualize, imagine a 2D grid: the 8 pixel are the four at the sides of each square and the four at the corners.

of the matrices tractable and consists in further binning together the pixel values, which is commonly done in two main ways: either the number of bins is fixed or the width of the bins is fixed preceeding the discretization process. It should be evident that the results of the feature extraction procedure is heavily dependent on the choices made in all the steps that preceed it, main of which being the segmentation, the eventual re-discretization of the image leading to the algorithm used to compute the feature themselves. For this reason recently the International Biomarker Standardization Initiative (IBSI [32]) wrote a *"reference manual"* which details in depth the definitons of the features, description of data-processing procedures as well as a set of guidelines for reporting results. This was done in an attempt to reduce as much as possible the variability and lack of reproducibility of radiomic studies. In the past the main attention in radiological research was focused on improving machine performances and evaluating acquisition sequence technologies, however the great developements in artificial intelligence and performance of computers have brought a lot of attention to the field. Various papers, such as [15] and [3] have been written with the objective of presenting the general workflow. By design the topics in this thesis have been presented to resemble the general order of the pipeline, which can be summarised as:

- Data acquisition
- Definition of the Region Of Interest (ROI)
- Pre-processing
- Feature extraction
- Feature selection
- Classification

Another interesting possibility offered by the biomarkers computed following radiomics is the ability to quatify the differences between successive exams of the same patient. This specific branch of radiomics is called Delta-radiomics, referencing to the time differential that become the main focus of the analysis.
NON SAPREI SE VA BENE COSI' O BISOGNA AGGIUNGERE

ALTRI DETTAGLI

With this the theoretical background has been laid out and the thesis can finally proceed to practically and more specifically describing the data at hand as well as the specific techniques used to elaborate it.

2.2 Data and objective

The objective of this thesis will be to compare how different methods perform in predicting clinical outcomes in covid patients, while also determining if different kind of input data imply different performances of the same methods. All images are non segmented, as such all of them are going to be semi-automatically segmented via a new software being tested in the medical physics department called *Sophia Radiomics*, which will be briefly explained shortly. Statistical analysis are going to be performed mainly in python using libraries such as scikit-learn, pandas, numpy, scipy while the graphical part of the analysis is done with either seaborn or matplotlib. The starting dataset was a list of all the patients that, from 02/2020 to 05/2021, were hospitalized as COVID-19 positive inside the facilities of *Azienda ospedaliero-universitaria di Bologna - Policlinico Sant'Orsola-Malpighi.* As far as exclusion criteria go the main exclusion criteria, except unavailability of the feature related to the patient, was visibly damaged or lower quality images, for example images with cropped lungs. The first set of selection criteria were:

- All patients that had undergone a CT exam which was retrievable via the PACS (Picture Archiving and Communication System) of *Azienda ospedaliero-universitaria di Bologna - Policlinico Sant'Orsola-Malpighi*
- All patients that had a all of the clinical and laboratory features, listed in fig:2.15, suggested by Lidia Strigari [30]

[30] She is, as of the writing of this thesis, the head of the Medical Physics department in the S. Orsola hospital. These suggestions were given to her by clinical professionals.

- Since all patient had at least 2 CT exams only the closest date to the hospital admission date was taken. When more exams were performed on the same date all of them were initially taken. At first only chest or abdomen CTs were taken regardless of the acquisition protocol used.

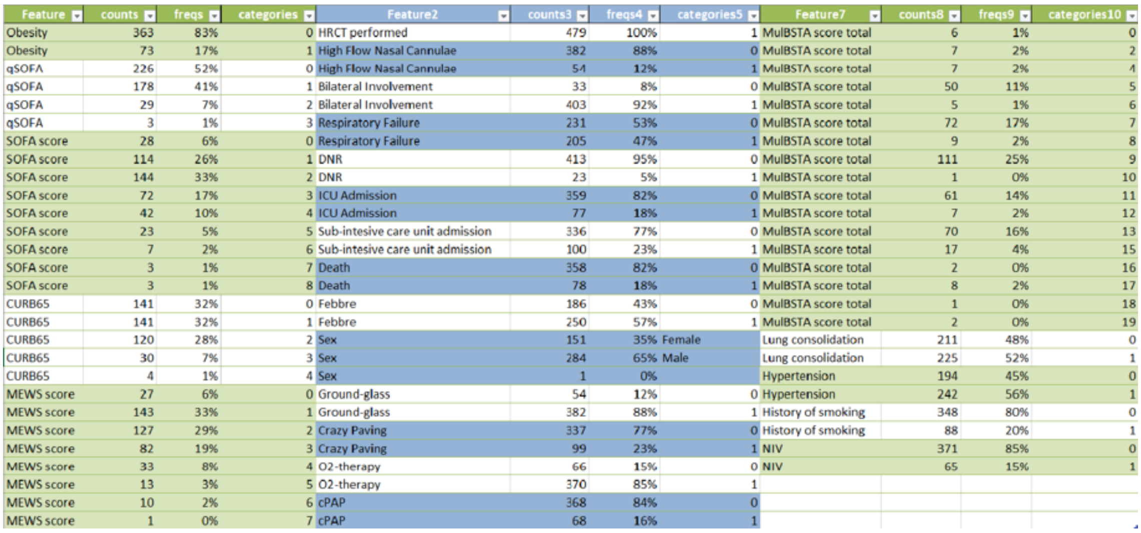

Feature	counts	freqs	categories	Feature2	counts3	freqs4	categories5	Feature7	counts8	freqs9	categories10
Obesity	363	83%	0	HRCT performed	479	100%	1	MulBSTA score total	6	1%	0
Obesity	73	17%	1	High Flow Nasal Cannulae	382	88%	0	MulBSTA score total	7	2%	2
qSOFA	226	52%	0	High Flow Nasal Cannulae	54	12%	1	MulBSTA score total	7	2%	4
qSOFA	178	41%	1	Bilateral Involvement	33	8%	0	MulBSTA score total	50	11%	5
qSOFA	29	7%	2	Bilateral Involvement	403	92%	1	MulBSTA score total	5	1%	6
qSOFA	3	1%	3	Respiratory Failure	231	53%	0	MulBSTA score total	72	17%	7
SOFA score	28	6%	0	Respiratory Failure	205	47%	1	MulBSTA score total	9	2%	8
SOFA score	114	26%	1	DNR	413	95%	0	MulBSTA score total	111	25%	9
SOFA score	144	33%	2	DNR	23	5%	1	MulBSTA score total	1	0%	10
SOFA score	72	17%	3	ICU Admission	359	82%	0	MulBSTA score total	61	14%	11
SOFA score	42	10%	4	ICU Admission	77	18%	1	MulBSTA score total	7	2%	12
SOFA score	23	5%	5	Sub-intesive care unit admission	336	77%	0	MulBSTA score total	70	16%	13
SOFA score	7	2%	6	Sub-intesive care unit admission	100	23%	1	MulBSTA score total	17	4%	15
SOFA score	3	1%	7	Death	358	82%	0	MulBSTA score total	2	0%	16
SOFA score	3	1%	8	Death	78	18%	1	MulBSTA score total	8	2%	17
CURB65	141	32%	0	Febbre	186	43%	0	MulBSTA score total	1	0%	18
CURB65	141	32%	1	Febbre	250	57%	1	MulBSTA score total	2	0%	19
CURB65	120	28%	2	Sex	151	35%	Female	Lung consolidation	211	48%	0
CURB65	30	7%	3	Sex	284	65%	Male	Lung consolidation	225	52%	1
CURB65	4	1%	4	Sex	1	0%		Hypertension	194	45%	0
MEWS score	27	6%	0	Ground-glass	54	12%	0	Hypertension	242	56%	1
MEWS score	143	33%	1	Ground-glass	382	88%	1	History of smoking	348	80%	0
MEWS score	127	29%	2	Crazy Paving	337	77%	0	History of smoking	88	20%	1
MEWS score	82	19%	3	Crazy Paving	99	23%	1	NIV	371	85%	0
MEWS score	33	8%	4	O2-therapy	66	15%	0	NIV	65	15%	1
MEWS score	13	3%	5	O2-therapy	370	85%	1				
MEWS score	10	2%	6	cPAP	368	84%	0				
MEWS score	1	0%	7	cPAP	68	16%	1				

Figure 2.15: Description of clinical label dataset, in sets of four columns there's the clinical feature, the total count of occurences, the percentage over the final dataset and the possible values the feature could take

Most clinical features are pretty self-explanatory, for those that were obscure to me as an outsider and not otherwise explained in **??**, I'm going to provide a very simple explanation:

1. DNR : Acronym for "Do Not Resuscitate", used to indicate the wish of the patient or their relatives that cardiac massage not be performed in case of cardiac arrest.

2. NIV: Acronym for "Non Invasive Ventilation", it's a form of respiratory aid provided to patients.

3. cPAP: Acronym for "continuous Positive Airway Pressure", another form of respiratory aid.

4. ICU: Acronym for "Intensive Care Unit". When patients are in really severe conditions they are treated in these facilities.

5. Clinical Scores: When available values from laboratory analyses and/or patient conditions are summarised in scores that represent the gravity of the state of the patient, as such these can be somewhat correlated and will be treated as comprehensive values to substitute an otherwise large set of obscure clinical features. At admission, or closely thereafter, a set of clinical questions regarding the patient receives a yes or no answer, each answer has an additive contribution towards the final value of the score.These scores differ in how much they add for each condition and the set of symptoms the check for.

   (a) MulBSTA: This score acconts for **Mul**tilobe lung involvement, absolute **L**ymphocyte count, **B**acterial coinfection, history of **S**moking, history of hyper**T**ension and **A**ge over 60 yrs. [10]

   (b) MEWS: Modified Early Warning Score for clinical deterioration. Computed considering systolic blood pressure, heart rate, respiratory rate, temperature and AVPU(Alert Voice Pain Unresponsive) score. [28]

   (c) CURB65: **C**onfusion, blood **U**rea Nitrogen or Urea level, **R**espiratory Rate, **B**lood pressure, age over **65** years. This score is specific for pneumonia severity [31]

   (d) SOFA: **S**equential **O**rgan **F**ailure **A**ssessment score. Considers various quantities from all systems to assess the overall state of the patient, PaO_2/FiO_2[31] for respiratory system, Glasgow Coma scale[32] for nervous, mean pressure for cardiovascular, Bilirubin levels for liver, platelets for coagulation and creatine for kidneys [2]

   (e) qSOFA: **q**uick SOFA. Only considers pressure, high respiratory rate and the low values in the Glasgow scale.

This procedure produced a starting cohort of ∼700 patients which, having all various images available, created a huge set of ∼2200 CT scans. Since this analysis is focused on radiomics there is an evident

[31] Very unrefined yet widely used indicator for lung disfunction

[32] GCS for short, proposed in 1974 by Graham Teasdale and Bryan Jennet. Evaluates what kind of stymulus is necessary to obtain motor and verbal reactions in the patient as well as what's necessary for the patient to open their eyes

need for as much consistency as possible in the images analysed. For this reason all CTs taken with medium of contrast were excluded, since they would have brightnesses not indicative of the disease, and for every patient only images with thin slice reconstruction were considered. More specifically only images with slice thickness of 1 o 1.25 mm[33] along the z-axis were taken into consideration, which meant excluding all the 1.5,2,2.5 and 5 mm slice thicknesses. Since all these images were segmented by me and two other students using a semiautomatic segmentation tool provided by the hospital it sometimes happened that manual corrections were necessary, these were performed only in very obvious and simple cases while, in all remaining cases, the patient was dropped out of the study. Overall this left the final study cohort to be composed of 435 patients, all descriptions and analyses are related to this cohort. The same software used for segmentation allowed the extraction of the radiomic features form the segmented volumes, even if it did not allow the extraction of the segmentation masks nor any changes in the segmentation parameters, which seems a region growth algorithm mixed with thresholding. For this reason all the image analysis in this thesis is reliant on said software which has been treated as a black-box. NON SO SE POSSO SCRIVERE CHE IL PROGRAMMA ERA DELUDENTE NE' QUANTO POSSO SBILANCIARMI A DARE INFO CHE NON HO SULLA SEGMENTAZIONE, SE CON LA STRIGARI HANNO PUBBLICATO L'ARTICOLO SULLA IBSI-COMPLIANCE SI POTREBBE CITARE QUELLO So, having segmented all the images and extracted all the features supported in the software, the next step is the definition of the actual analysis pipeline. The whole dataset was comprised of ∼200 features, which were divided in three subgroups as follows:

1. Clinical: All these features are derived from the admission pro-

[33] This meant that only exams called 'Parenchima' or 'HRCT' were included. Throughout the internship 'parenchima' has always appeared in contrast with 'mediastino'. These two keywords are used in the phase of reconstruction of the raw data to identify reconstructions with specific properties. Parenchima is used for finer reconstruction of lung specifically, the requiring professional uses these images to look for small nodules with very high contrast and, to do so, the reconstruction allows some noise to achieve the best resolution possible. Mediastino is used in the lung, as well as other regions, to look for bigger lesions but with low contrast. As such the 'mediastino' reconstruction compromises a worse spatial resolution for a better display of contrast, visually speaking the first images are more coarse and noisy while the second are smoother. It should be noted that even with the same identifier, be it HRCT parenchima or others, the machines on which the exams were made were different and had different proprietary convolutional kernels used for reconstruction.

cedure in the hospital.

- The continuous are Age taken at the date of the CT exam and Respiratory Rate defined as number of breaths in a minute.
- The discrete one were the aforementioned scores and the boolean ones were sex of the patient, obesity status, if the patient had a fever[34] as of hospital admission and whether or not the patient suffered of Hypertension
- The remaining features, namely those in 2.2 as well as the death status of the patient, were wither used as labels or not used at all because they refer to treatments used and not characteristics of the patient. As such these features, while plausibly correlated to the clinical outcome, are not really descriptive of the patient as of admission and are not information that can be used to aid professionals at admission to assess the situation

2. Radiomic: These features were all the ones supported by the segmentation software and are pretty much most of those described in [32] with the addition of fat and muscle surface, computed as cm^2 by counting pixel identified via threshold as fat or muscle tissue in thoracic slices taken at height of vertebra T-12

3. Radiological: These features are those that can be derived from CT exams by humas. Namely acquisition parameters, such as KVP and Current, were used to search for eventual correlations between image quality and predictive power of the feature derived from the image while boolean features, such as Bilaterality of lung damage, presence of Groun Glass Opacities (GGO), lung consolidations as well as crazy paving were used to see if they were sufficient in determining outcome.

2.3 Preprocessing and data analysis

Before any preprocessing a choice was made to exclude all of the clinical scores, this was done to avoid having them mask other, more

[34] Defined as body temperature>38°

straightforward variables. **QUESTO ANDRA MESSO IN UNA FOOTNOTE**In **APPENDICE SE MAI RIESCO A SCRIVERLA** an alternative choice will be made, namely to keep only the most strongly predicting one out of all of them. The first step in the analysis of this data is going to be a lasso regularized regression using either death or ICU admission as target. As mentioned before when operationg with regressions it's a necessity that the residuals be normally distributed, a common way to get as close as possible to this hypothesis is to boxcox transform the data. Apart from the data which contained negative values, which cannot be fed into the boxcox transform, all variables have been transformed using this method.

The quatile-quantile plots have been used for a visual check of normality, normally distributed data will populate the bisector of the graph while deviations are symptoms of non-normality. Heavy and light tails are visible as deviations respectively above and belox the bisector. It should be noted that when the data is normally distributed then the transform doesn't change much the distribution while, in cases with more heavy tailed distributions, the improvement is clear to see as it can be seen in Figures 2.16 and 2.17 The next preprocessing step has been to apply a *StandardScaler* to all of the features, which corresponds to subtracting the mean and dividing by the standard deviation, in order to center all the features around zero. The final step in preprocessing has been to reduce the features by using a correlation threshold which means that all variables that correlate with another more, in absolute value, than a certain threshold, which has been set to 0.6 in this work, are dropped a priori. A rather important thing to notice is that correlation has been computed using Spearman correlation and not Pearson since the first is invariant under monotone transformations, such as boxcox, and the second is not. Given the large number of features it's very plausible that at least one of the eliminated features is correlated with all other dropped features but with none of the remaing ones, since a Lasso regularization will be used introducing a few redundant features is not too damaging and the possible benefits outweight the risks. For this reason a redrawing method has been implemented to add one of the dropped features, this has been done by choosing the one that most correlates with the label being used. A pivotal point in all of this analysis is

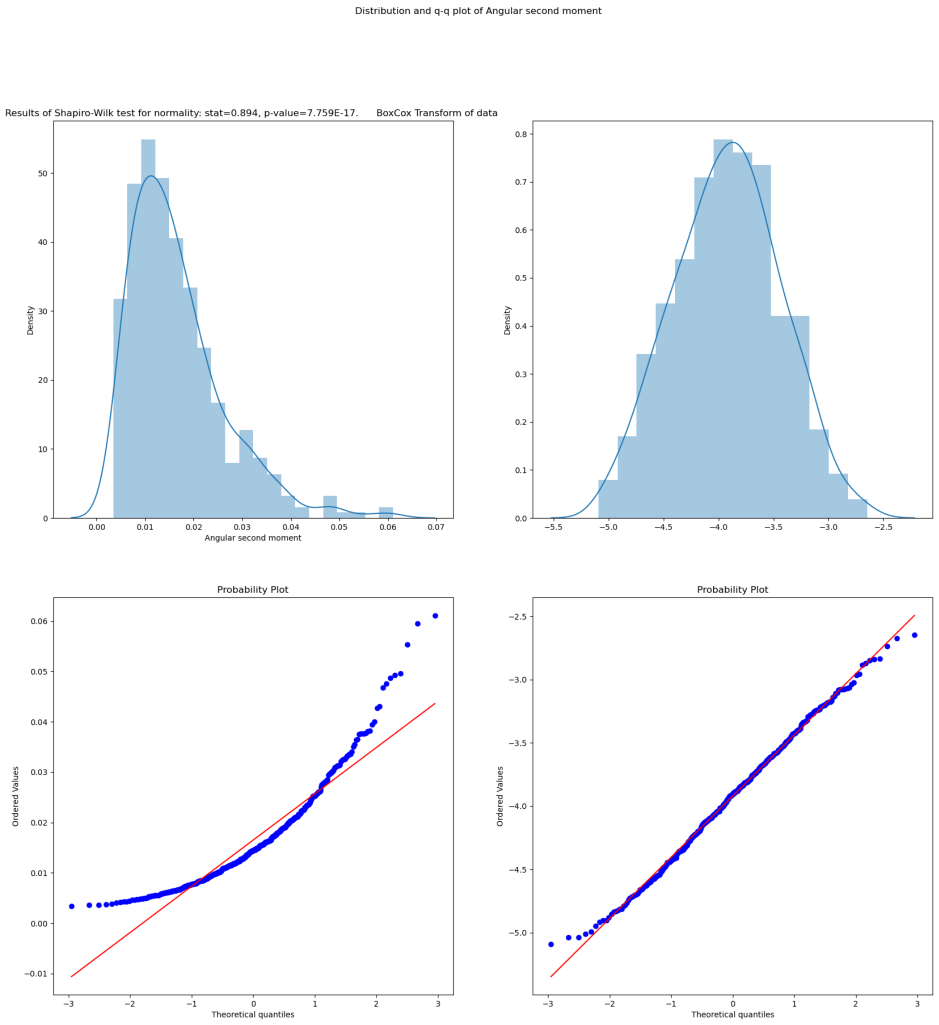

Figure 2.16: Example of boxcox applied to the radiomic feature *Angular second moment* which has a heavy tailed distribution. The graphs contain the original distribution (top-left) the transformed distribution (top-right) and the two respective quantile-quantile plots

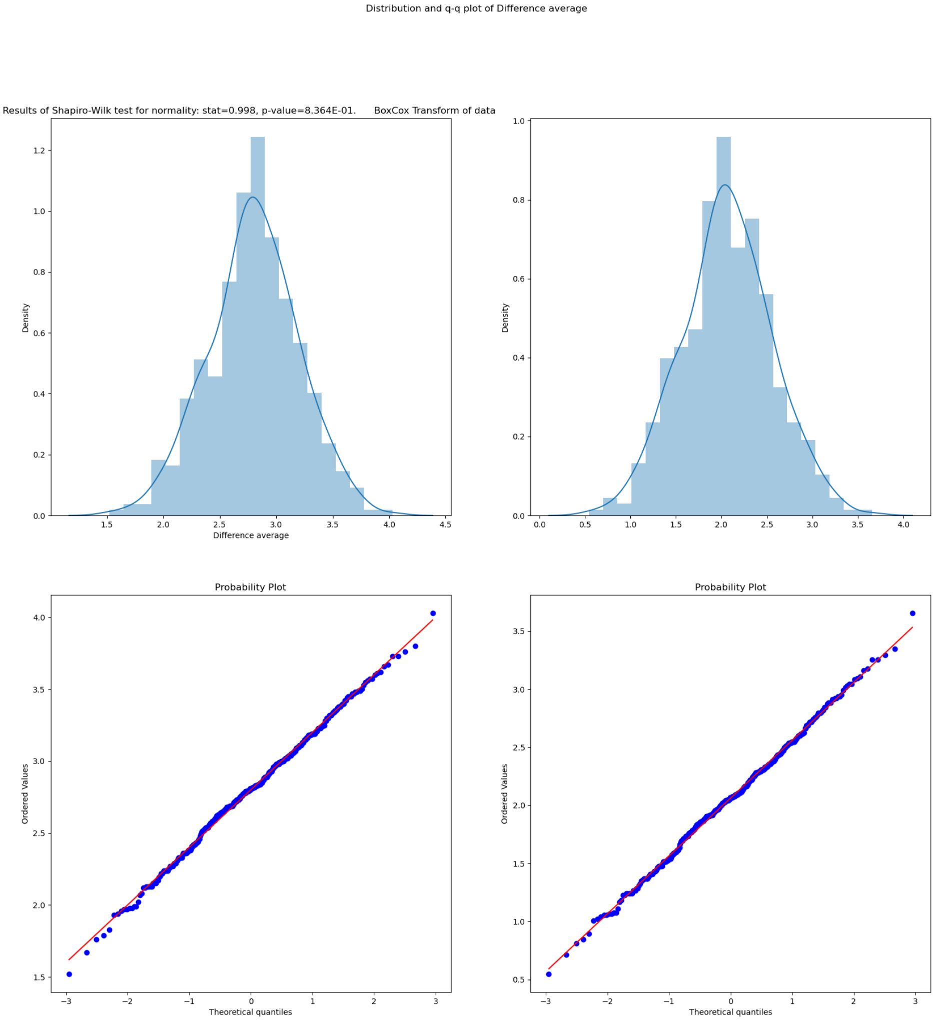

Figure 2.17: Example of boxcox applied to the radiomic feature *Difference Average* which has a close to normal distribution. The graphs contain the original distribution (top-left) the transformed distribution (top-right) and the two respective quantile-quantile plots

that, to obtain reasonable values in the cross-validation procedures and to avoid leakage[35] problems, all of the preprocessing steps have been done after train-test splitting the data on the train set and then applied as defined during training on the test dataset. When it comes to cross-validation procedure the choice was made to use a stratified k-fold approach with k=10, the data is split in 10 parts with the same percentages of labels[36] then a model is built by training on 9 of the folds and it's performance is then tested on the remaining fold. To use the whole dataset for testing a prediction of it has been built by combinig the predictions on the 10^{th}" fold for ten different models trained on the respective 9 remaining folds. The lasso model from training on the 9 folds is actually chosen as the model with the hyperparameters that give the best performance with another 10-fold crossvalidation. This has been obtained by using *cross_val_predict* on a model obtained by including a *LassoCV* step inside a *pipeline* from scikit-learn library in python. The performance of the cross-validated predictions that, when built this way, is much more representative of the real-world performance of the model, has been evaluated using ROC curves and AUC. Different models have been compared with a Delong test[7] for the significance of difference in the ROC curves.

The second analysis method used was RandomForest. As said before in this case no preprocessing was needed nor has been done, however particular care was taken in handling the imbalances in the dataset by using SMOTE [6] once again being careful to avoid leakage. The performance of this model was evaluated using confusion matrices which, at a glance, provide very much information on the situation of the data.

Finally a few dimensionality reduction techniques, namely the unsupervised PCA[8] and Umap [19] and the supervised PLS-DA[4], have been used to understand better the state of the data and further explain some of the obtained results.

This concludes the discussion on the methodologies used and leads

[35] This term is used in the field of Machine Learning. It refers to models being created on information that comes from outside the training data.

[36] The stratified in the name refers to this property. This method is useful when dealing with unbalanced datasets, such the one under analysis, in which the label has an uneven 15-85% frequency of occurences of the two labels

perfectly in the discussion of the results.

Chapter 3

Results

By performing a lasso and building a predicting score as sum of features multiplied by their importance derived from the lasso we obtain the following results. Note that the features are being kept separated.

3.1 LASSO

3.1.1 Death

3.1.2 ICU Admission

3.2 Ramdom forest

3.2.1 Death

3.2.2 ICU Admission

3.3 Dimensionality reduction

RAD

	Lasso Importance
Intensity-based interquartile range	0.153884
10th discretised intensity percentile	-0.113928
Complexity	-0.060896
Cluster prominence	-0.057964
Area density - aligned bounding box	-0.045552
Asphericity	0.025736
Number of compartments (GMM)	-0.023584
Local intensity peak	0.022764
Global intensity peak	-0.020052
Entropy	0.001594

CLINICHE

Feature Name	Lasso Importance
CURB65	0.125837
Respiratory Rate	0.044918
Ground-glass	-0.032842
Age (years)	0.022695
Lung consolidation	0.021103
Crazy Paving	-0.003770

CLINICHE + RADIOMICHE

Feature Name	Lasso Importance
CURB65	0.106256
Intensity histogram quartile coefficient of dis...	0.067802
Cluster shade	-0.031718
Area density - enclosing ellipsoid	-0.030894
Ground-glass	-0.030125
Respiratory Rate	0.018603
Centre of mass shift (cm)	0.016225
Normalised zone distance non-uniformity	0.016027
High dependence high grey level emphasis	0.012445
RECIST (cm)	0.012194
Lung consolidation	0.009602
Number of compartments (GMM)	-0.005958
Small distance high grey level emphasis	0.002856
Age (years)	0.002662
Local intensity peak	0.000458
Discretised interquartile range	0.000204

NUOVI RISULTATI CON CV MESSA A POSTO

model with features CLI predicting on Death

	Lasso Importance
Intercept	0.179310
Respiratory Failure	0.125539
CURB65	0.098730
NIV	0.063025
High Flow Nasal Cannulae	-0.054100
Age (years)	0.037878
Sex_bin	-0.030768
Respiratory Rate	0.029698
Hypertension	-0.025957
Febbre	-0.024351
History of smoking	-0.004735
O2-therapy	0.001422
cPAP	0.000000
Obesity	0.000000

model with features RAD predicting on Death

	Lasso Importance
Intercept	0.179310
10th intensity percentile	-0.135324
Intensity-based interquartile range	0.108819
Complexity	-0.106005
Cluster prominence	-0.071387
Area density - aligned bounding box	-0.043236
Number of compartments (GMM)	-0.032827
Entropy	0.032588
Asphericity	0.031313
Local intensity peak	0.029984
Global intensity peak	-0.024439
Intensity range	0.003523
Number of voxels of positive value	0.002876
Major axis length (cm)	0.000000

model with features RADIOLOGICHE predicting on Death

	Lasso Importance
Intercept	0.179310
Ground-glass	-0.043392
Lung consolidation	0.036983
KVP	0.006288
SliceThickness	0.000000
Bilateral Involvement	0.000000
Crazy Paving	-0.000000

model with features CLINICHE-RADIOMICHE predicting on Death

	Lasso Importance
Intercept	0.179310
Respiratory Failure	0.114018
CURB65	0.087693
NIV	0.066066
High Flow Nasal Cannulae	-0.052176
10th intensity percentile	-0.045649
Complexity	-0.045647
Age (years)	0.035750
Intensity-based interquartile range	0.033743
Cluster prominence	-0.033215
Hypertension	-0.029762
Febbre	-0.027388
Sex_bin	-0.021811
Local intensity peak	0.019209
Area density - aligned bounding box	-0.019154
Number of compartments (GMM)	-0.018901
Respiratory Rate	0.018730
Asphericity	0.011561
Global intensity peak	-0.011437
History of smoking	-0.006063
Number of voxels of positive value	-0.002575
Obesity	-0.000789
cPAP	0.000000
O2-therapy	0.000000
Intensity range	0.000000

model with features CLINICHE-RADIOLOGICHE predicting on Death

	Lasso Importance
Intercept	0.179310
Respiratory Failure	0.120194
CURB65	0.094263
NIV	0.057815
High Flow Nasal Cannulae	-0.043542
Age (years)	0.032253
Ground-glass	-0.030685
Respiratory Rate	0.024414
Sex_bin	-0.023705
Febbre	-0.022482
Lung consolidation	0.021949
Hypertension	-0.015673
KVP	0.010137
SliceThickness	0.008467
Crazy Paving	-0.004071
History of smoking	-0.002543
Bilateral Involvement	-0.000000
cPAP	0.000000
O2-therapy	0.000000
Obesity	-0.000000

model with features RADIOLOGICHE-RADIOMICHE predicting on Death

	Lasso Importance
Intercept	0.179310
Intensity-based interquartile range	0.134591
10th intensity percentile	-0.120165
Complexity	-0.092609
Cluster prominence	-0.072762
Ground-glass	-0.053392
Area density - aligned bounding box	-0.034919
Lung consolidation	0.033863
Asphericity	0.027229
Number of compartments (GMM)	-0.024474
Local intensity peak	0.022962
Global intensity peak	-0.016252
KVP	0.011303
Crazy Paving	-0.011005
Bilateral Involvement	-0.009681
Major axis length (cm)	0.003229
Intensity range	0.000000
Entropy	0.000000
Number of voxels of positive value	0.000000
SliceThickness	-0.000000

model with features ALL predicting on Death

	Lasso Importance
Intercept	0.179310
Respiratory Failure	0.110246
CURB65	0.087816
NIV	0.041397
Intensity-based interquartile range	0.036132
High Flow Nasal Cannulae	-0.030074
Ground-glass	-0.027476
Age (years)	0.021863
Complexity	-0.018867
Sex_bin	-0.018822
Febbre	-0.016067
Lung consolidation	0.014519
Cluster prominence	-0.011701
Respiratory Rate	0.009586
Number of compartments (GMM)	-0.005002
Hypertension	-0.004976
Area density - aligned bounding box	-0.003381
KVP	0.001906
Crazy Paving	-0.001778
History of smoking	-0.000000
Obesity	-0.000000
O2-therapy	0.000000
cPAP	0.000000
Intensity range	0.000000
SliceThickness	0.000000
Global intensity peak	-0.000000
Number of voxels of positive value	0.000000
10th intensity percentile	-0.000000
Asphericity	0.000000
Local intensity peak	0.000000
Bilateral Involvement	-0.000000

Risultati con il random forest classifier implementazione naive

Accuracy score= 0.832183908045977 RMSE= 0.40965362436334307

class	precision	recall	f1-score	support
0	0.84	0.98	0.91	357
1	0.65	0.14	0.23	78
accuracy			0.83	435
macro avg	0.74	0.56	0.57	435
weighted avg	0.81	0.83	0.78	435

feature	RF_importances
Respiratory Failure	0.073410
CURB65	0.048355
Age (years)	0.042183
Discretised interquartile range	0.015215
Normalised zone size non-uniformity	0.014503
Zone size entropy	0.013022
Intensity histogram quartile coefficient of dis...	0.012877
Dependence count entropy	0.012349
Intensity histogram robust mean absolute deviation	0.012038
Dependence count energy	0.011250
Information correlation 2	0.010936
Intensity-based interquartile range	0.010557
Intensity-based median absolute deviation	0.010335
Uniformity	0.010092
Normalised grey level non-uniformity (GLRLM)	0.009950
Entropy	0.009521
Skewness	0.009466
Respiratory Rate	0.009128
Run entropy	0.009112
Discretised intensity skewness	0.009056
Zone distance entropy	0.008693
Cluster prominence	0.008389
Large distance high grey level emphasis	0.008030
NIV	0.007973
XRayTubeCurrent	0.007913
Information correlation 1	0.007777
Discretised intensity entropy	0.007500
Intensity-based robust mean absolute deviation	0.007225
Angular second moment	0.007216
Centre of mass shift (cm)	0.007092
Thresholded area intensity peak (75%)	0.007058
Normalised grey level non-uniformity (GLSZM)	0.007012
Small distance emphasis	0.006851
Discretised intensity uniformity	0.006661
Energy	0.006559
Standard deviation	0.006534
Small zone emphasis	0.006514
Small distance high grey level emphasis	0.006364
Low grey level zone emphasis.1	0.006298
Normalised zone distance non-uniformity	0.006248
Minor axis length (cm)	0.006193
Volume density - enclosing ellipsoid	0.006183

2d embedding con umap dati non scalati prima di umap, su gravity con percentili 25-75 Accuracy score= 0.3586206896551724 RMSE= 1.2317635241028795

precision recall f1-score support

1 0.18 0.15 0.17 79 2 0.46 0.58 0.51 193 3 0.18 0.14 0.16 85 4 0.34 0.27 0.30 78

accuracy 0.36 435 macro avg 0.29 0.28 0.28 435 weighted avg 0.33 0.36 0.34 435

	RF_importances
1	0.508338
0	0.491662

2d embedding con umap dati scalati prima di umap, su gravity con percentili 25-75

Accuracy score= 0.4459770114942529 RMSE= 1.02721585550122

precision recall f1-score support

1 0.37 0.29 0.33 79 2 0.53 0.61 0.57 193 3 0.32 0.31 0.31 85 4 0.39 0.36 0.38 78

accuracy 0.45 435 macro avg 0.40 0.39 0.40 435 weighted avg 0.44 0.45 0.44 435

	RF_importances
0	0.530961
1	0.469039

RISULTATI CON FAT E MUSCLE)

lassocv with features CLI predicting on Death

	lassocvL1 penalty Importance
Intercept	0.179724
Respiratory Failure	0.128088
CURB65	0.102566
NIV	0.061168
High Flow Nasal Cannulae	-0.049616
Age (years)	0.031801
Respiratory Rate	0.024426
Hypertension	-0.023176
Febbre	-0.021664
Sex_bin	0.009949
History of smoking	-0.002102
O2-therapy	0.000486
Obesity	-0.000000
cPAP	0.000000

lassocv with features RAD predicting on Death

	lassocvL1 penalty Importance
Intercept	0.179723
10th intensity percentile	-0.129937
Complexity	-0.106041
Intensity-based interquartile range	0.105169
Cluster prominence	-0.067630
Area density - aligned bounding box	-0.039259
Entropy	0.035969
Number of compartments (GMM)	-0.033142
Local intensity peak	0.029582
Asphericity	0.028715
Global intensity peak	-0.025238
Intensity range	0.009107
Fat.surface	0.008150
Number of voxels of positive value	0.000258
Major axis length (cm)	0.000000

lassocv with features RADIOLOGICHE predicting on Death

	lassocvL1 penalty Importance
Intercept	0.179724
Ground-glass	-0.043786
Lung consolidation	0.039074
XRayTubeCurrent	-0.016411
KVP	0.005251
Crazy Paving	-0.000000
Bilateral Involvement	0.000000
SliceThickness	0.000000

lassocv with features CLIRAD predicting on Death

	lassocvL1 penalty Importance
Intercept	0.179724
Respiratory Failure	0.118604
CURB65	0.088668
NIV	0.069345
High Flow Nasal Cannulae	-0.050231
Complexity	-0.048003
10th intensity percentile	-0.040592
Age (years)	0.039638
Hypertension	-0.032531
Area density - aligned bounding box	-0.031491
Cluster prominence	-0.028555
Febbre	-0.027227
Respiratory Rate	0.023872
Asphericity	0.022113
Sex_bin	0.020739
Local intensity peak	0.019734
Number of compartments (GMM)	-0.016025
Global intensity peak	-0.010200
History of smoking	-0.006554
Fat.surface	0.004962
Obesity	-0.002121
cPAP	0.001717
O2-therapy	0.001134
Intensity range	0.000000
Major axis length (cm)	0.000000
Number of voxels of positive value	0.000000

lassocv with features CLIRADIOLOGICHE predicting on Death

	lassocvL1 penalty Importance
Intercept	0.179724
Respiratory Failure	0.122234
CURB65	0.096522
NIV	0.058161
High Flow Nasal Cannulae	-0.041193
Ground-glass	-0.030321
Age (years)	0.028157
Lung consolidation	0.023424
Respiratory Rate	0.023238
Febbre	-0.020553
Hypertension	-0.014563
SliceThickness	0.011240
KVP	0.009409
Sex_bin	0.007833
Crazy Paving	-0.006860
XRayTubeCurrent	-0.005432
History of smoking	-0.001715
O2-therapy	0.000000
cPAP	0.000000
Bilateral Involvement	-0.000000
Obesity	-0.000000

lassocv with features RADIOLOGICHE-RAD predicting on Death

	lassocvL1 penalty Importance
Intercept	0.179724
Intensity-based interquartile range	0.132780
10th intensity percentile	-0.101479
Complexity	-0.084790
Cluster prominence	-0.067690
XRayTubeCurrent	-0.057481
Ground-glass	-0.053869
Lung consolidation	0.032543
Area density - aligned bounding box	-0.032283
Fat.surface	0.027230
Local intensity peak	0.025490
Asphericity	0.024992
Number of compartments (GMM)	-0.022803
Major axis length (cm)	0.015081
Global intensity peak	-0.013740
Crazy Paving	-0.013243
SliceThickness	0.009068
Bilateral Involvement	-0.007472
Number of voxels of positive value	0.002466
KVP	0.000967
Intensity range	0.000000

lassocv with features ALL predicting on Death.

	lassocvL1 penalty Importance
Intercept	0.179724
Respiratory Failure	0.113546
CURB65	0.090561
NIV	0.045254
High Flow Nasal Cannulae	-0.030218
Ground-glass	-0.028004
Complexity	-0.027004
Age (years)	0.021476
Lung consolidation	0.018403
Febbre	-0.016850
Intensity-based interquartile range	0.016214
Respiratory Rate	0.012148
XRayTubeCurrent	-0.012029
Cluster prominence	-0.010913
Fat.surface	0.010110
Hypertension	-0.008660
Area density - aligned bounding box	-0.008552
Sex_bin	0.005420
Number of compartments (GMM)	-0.003722
KVP	0.003274
Crazy Paving	-0.003203
Local intensity peak	0.002753
Major axis length (cm)	0.000099
cPAP	0.000000
Number of voxels of positive value	-0.000000
Intensity range	0.000000
O2-therapy	0.000000
Asphericity	0.000000
Obesity	-0.000000
Bilateral Involvement	-0.000000
SliceThickness	0.000000
10th intensity percentile	-0.000000
History of smoking	-0.000000
Global intensity peak	-0.000000

USANDO ANCHE FAT E MUSCLE SURFACE

lassocv with features CLI predicting on ICU Admission

	lassocvL1 penalty Importance
NIV	0.217471
Intercept	0.177419
Respiratory Failure	0.050953
High Flow Nasal Cannulae	0.015014
Febbre	0.009632
History of smoking	0.002855
Sex_bin	-0.001857
Age (years)	-0.000000
Hypertension	0.000000
Obesity	0.000000
O2-therapy	0.000000
cPAP	-0.000000
Respiratory Rate	0.000000
CURB65	-0.000000

lassocv with features RAD predicting on ICU Admission

	lassocvL1 penalty Importance
Intercept	0.177419
Number of voxels of positive value	0.159984
Intensity range	-0.147273
Entropy	0.136924
Cluster prominence	-0.122875
Complexity	-0.097204
10th intensity percentile	-0.083223
Area density - aligned bounding box	-0.035995
Major axis length (cm)	-0.034635
Dependence count entropy	-0.034174
Fat.surface	0.028454
Asphericity	-0.024527
Local intensity peak	-0.019615
Global intensity peak	-0.015779
Number of compartments (GMM)	-0.000045

lassocv with features RADIOLOGICHE predicting on ICU Admission

	lassocvL1 penalty Importance
Intercept	1.774194e-01
XRayTubeCurrent	4.092988e-18
Lung consolidation	0.000000e+00
Ground-glass	0.000000e+00
Crazy Paving	0.000000e+00
Bilateral Involvement	0.000000e+00
SliceThickness	-0.000000e+00
KVP	0.000000e+00

lassocv with features CLIRAD predicting on ICU Admission

	lassocvL1 penalty Importance
NIV	0.209694
Intercept	0.177419
Intensity range	-0.096034
Number of voxels of positive value	0.094488
Cluster prominence	-0.085690
Respiratory Failure	0.060791
Complexity	-0.049243
Major axis length (cm)	-0.043330
10th intensity percentile	-0.040822
High Flow Nasal Cannulae	0.029217
Area density - aligned bounding box	-0.026951
cPAP	-0.025035
Febbre	0.023916
Dependence count entropy	0.020979
History of smoking	0.020918
Age (years)	-0.019277
Local intensity peak	-0.017481
Sex_bin	-0.013865
Hypertension	0.012981
O2-therapy	0.008794
Fat.surface	-0.008065
Asphericity	0.006228
Obesity	0.003853
Global intensity peak	-0.000495
Number of compartments (GMM)	0.000352
Respiratory Rate	-0.000000

lassocv with features CLIRADIOLOGICHE predicting on ICU Admission

	lassocvL1 penalty Importance
NIV	0.218300
Intercept	0.177419
Respiratory Failure	0.053616
High Flow Nasal Cannulae	0.018061
SliceThickness	0.012860
Febbre	0.011785
History of smoking	0.005857
Sex_bin	-0.004416
Age (years)	-0.004101
O2-therapy	0.001615
CURB65	0.000000
Respiratory Rate	0.000000
Lung consolidation	0.000000
cPAP	-0.000000
Ground-glass	0.000000
Hypertension	0.000000
XRayTubeCurrent	0.000000
KVP	0.000000
Bilateral Involvement	-0.000000
Crazy Paving	-0.000000
Obesity	0.000000

lassocv with features RADIOLOGICHE-RAD predicting on ICU Admission

	lassocvL1 penalty Importance
Intercept	0.177419
Dependence count entropy	0.066657
Number of voxels of positive value	0.022742
Fat.surface	0.015496
Complexity	-0.000000
Number of compartments (GMM)	0.000000
Major axis length (cm)	0.000000
Local intensity peak	-0.000000
Intensity range	-0.000000
Global intensity peak	-0.000000
Lung consolidation	-0.000000
Ground-glass	0.000000
Asphericity	-0.000000
Area density - aligned bounding box	-0.000000
10th intensity percentile	0.000000
XRayTubeCurrent	0.000000
KVP	0.000000
SliceThickness	-0.000000
Bilateral Involvement	-0.000000
Crazy Paving	0.000000
Cluster prominence	-0.000000

lassocv with features ALL predicting on ICU Admission

	lassocvL1 penalty Importance
NIV	0.213070
Intercept	0.177419
Respiratory Failure	0.042212
Complexity	-0.023928
High Flow Nasal Cannulae	0.020592
Dependence count entropy	0.013990
Febbre	0.007409
History of smoking	0.000389
O2-therapy	0.000000
Major axis length (cm)	0.000000
XRayTubeCurrent	0.000000
KVP	0.000000
SliceThickness	0.000000
Bilateral Involvement	-0.000000
Crazy Paving	-0.000000
Ground-glass	0.000000
Lung consolidation	-0.000000
Fat.surface	0.000000
Number of voxels of positive value	0.000000
Number of compartments (GMM)	-0.000000
Intensity range	-0.000000
Local intensity peak	-0.000000
cPAP	-0.000000
Global intensity peak	-0.000000
Hypertension	0.000000
Cluster prominence	-0.000000
Asphericity	0.000000
Area density - aligned bounding box	-0.000000
10th intensity percentile	0.000000
Sex_bin	-0.000000
Respiratory Rate	0.000000
Obesity	0.000000
Age (years)	-0.000000

Bibliography

[1] Nema ps3 / iso 12052, digital imaging and communications in medicine (dicom) standard, national electrical manufacturers association, rosslyn, va, usa. available free at, 2021.

[2] J. L. V. 1, R. Moreno, J. Takala, S. Willatts, A. D. Mendonça, H. Bruining, C. K. Reinhart, P. M. Suter, and L. G. Thijs. The sofa (sepsis-related organ failure assessment) score to describe organ dysfunction/failure. on behalf of the working group on sepsis-related problems of the european society of intensive care medicine. *Intensive Care Medicine*, 1996.

[3] U. Attenberger and G. Langs. How does radiomics actually work? – review. *RöFo - Fortschritte auf dem Gebiet der Röntgenstrahlen und der bildgebenden Verfahren*, 193, 12 2020.

[4] M. Barker and W. Rayens. Partial least squares for discrimination, journal of chemometrics. *Journal of Chemometrics*, 17:166 – 173, 03 2003.

[5] R. W. Brown, Y.-C. N. Cheng, E. M. Haacke, M. R. Thompson, and R. Venkatesan. *Magnetic Resonance Imaging: Physical Principles and Sequence Design, 2nd Edition*. Wiley-Blackwell, 2014.

[6] N. V. Chawla, K. W. Bowyer, L. O. Hall, and W. P. Kegelmeyer. Smote: Synthetic minority over-sampling technique. *Journal of Artificial Intelligence Research*, 16:321–357, Jun 2002.

[7] E. R. DeLong, D. M. DeLong, and D. L. Clarke-Pearson. Comparing the areas under two or more correlated receiver operating characteristic curves: A nonparametric approach. *Biometrics*, 44(3):837–845, 1988.

[8] K. P. F.R.S. Liii. on lines and planes of closest fit to systems of points in space. *The London, Edinburgh, and Dublin Philosophical Magazine and Journal of Science*, 2(11):559–572, 1901.

[9] D. G. George H. Joblove. Color spaces for computer graphics. *ACM SIGGRAPH Computer Graphics*, (12(3), 20–25), 1978.

[10] L. Guo. Clinical features predicting mortality risk in patients with viral pneumonia: The mulbsta score. *Frontiers in Microbiology*, 2019.

[11] G. N. Hounsfield. Computed medical imaging. nobel lecture. *Journal of Computer Assisted Tomography*, (4(5):665-74), 1980.

[12] L. M. J. Cine computerized tomography. *The International Journal of Cardiac Imaging*, 1987.

[13] A. Kaka and M. Slaney. *Principles of Computerized Tomographic Imaging*. Society of Industrial and Applied Mathematics, 2001.

[14] J. Kirby. Mosmeddata: dataset, 09/2021.

[15] P. Lambin, R. T. H. Leijenaar, T. M. Deist, J. Peerlings, E. E. C. de Jong, J. van Timmeren, S. Sanduleanu, R. T. H. M. Larue, A. J. G. Even, A. Jochems, Y. van Wijk, H. Woodruff, J. van Soest, T. Lustberg, E. Roelofs, W. van Elmpt, A. Dekker, F. M. Mottaghy, J. E. Wildberger, and S. Walsh. Radiomics: the bridge between medical imaging and personalized medicine. *Nature reviews. Clinical oncology*, 14(12):749—762, December 2017.

[16] L. Lee and C.-Y. Liong. Partial least squares-discriminant analysis (pls-da) for classification of high-dimensional (hd) data: a review of contemporary practice strategies and knowledge gaps. *The Analyst*, 143, 06 2018.

[17] G. Lemaître, F. Nogueira, and C. K. Aridas. Imbalanced-learn: A python toolbox to tackle the curse of imbalanced datasets in machine learning. *Journal of Machine Learning Research*, 18(17):1–5, 2017.

[18] J. McCarthy. What is artificial intelligence? 01 2004.

[19] L. McInnes, J. Healy, and J. Melville. Umap: Uniform manifold approximation and projection for dimension reduction, 2020.

[20] S. J. McMahon. The linear quadratic model: usage, interpretation and challenges. *Physics in medicine and biology*, 2018.

[21] S. Morozov. Mosmeddata: Chest ct scans with covid-19 related findings dataset. *IAU Symp.*, (S227), 2020.

[22] MosMed. Mosmeddata: dataset, 28/04/2020.

[23] Y. Ohno. Cie fundamentals for color measurements. *International Conference on Digital Printing Technologies*, 01 2000.

[24] D. L. Pham, C. Xu, and J. L. Prince. Current methods in medical image segmentation. *Annual Review of Biomedical Engineering*, 2(1):315–337, 2000. PMID: 11701515.

[25] P. C. Rajandeep Kaur. A review of image compression techniques. *International Journal of Computer Applications*, 2016.

[26] W. C. Roentgen. On a new kind of rays. *Science*, 1986.

[27] A. Saltelli. *Global Sensitivity Analysis. The Primer.* John Wiley and Sons, Ltd, 2007.

[28] C. P. Subbe. Validation of a modified early warning score in medical admissions. *QJM: An international journal of medicine*, 2001.

[29] L. Tommy. Gray-level invariant haralick texture features. *PLOS ONE*, 2019.

[30] S. Webb. The physics of medical imaging. 1988.

[31] L. WS, van der Eerden MM, and e. a. Laing R. Defining community acquired pneumonia severity on presentation to hospital: an international derivation and validation study. *Thorax 58(5):377-382*, 2003.

[32] A. Zwanenburg, M. Vallières, M. A. Abdalah, H. J. W. L. Aerts, V. Andrearczyk, A. Apte, S. Ashrafinia, S. Bakas, R. J. Beukinga, R. Boellaard, and et al. The image biomarker standardization initiative: Standardized quantitative radiomics for high-throughput image-based phenotyping. *Radiology*, 295(2):328–338, May 2020.